NEUTRALINOS AND THE ORIGIN OF RADIO HALOS IN CLUSTERS OF GALAXIES

S. COLAFRANCESCO

Osservatorio Astronomico di Roma, Via Frascati, 33, I-00040

Monteporzio - ITALY

Email: cola@coma.mporzio.astro.it

and

B. MELE

INFN, Sezione di Roma, and University of Rome "La Sapienza"

Rome - ITALY

Email: Barbara.Mele@roma1.infn.it

Received _____; accepted _____

ABSTRACT

We assume that the supersymmetric lightest neutralino is a good candidate for the cold dark matter in the galaxy halo, and explore the possibility to produce extended diffuse radio emission from high-energy electrons arising from the neutralino annihilation in galaxy clusters whose intracluster medium is filled with a large-scale magnetic field. We show that these electrons fit the population of seed relativistic electrons that is postulated in many models for the origin of cluster radio halos. If the magnetic field has a central value of $3 \div 30$ μG (depending on the Dark Matter profile) and is radially decreasing from the cluster center, the population of seed relativistic electrons from neutralino annihilation can fit the radio halo spectra of two well studied cluster: Coma and 1E0657-56. The shape and the frequency extension of the radio halo spectra are connected with the mass and physical composition of the neutralino. A pure-gaugino neutralino with mass $M_\chi \geq 80$ GeV can reasonably fit the radio halo spectra of both Coma and 1E0657-56. This model provides a number of extra predictions that make it definitely testable. On the one hand, it agrees quite well with the observations that *(i)* the radio halo is centered on the cluster dynamical center, usually coincident with the center of its X-ray emission, *(ii)* the radio halo surface brightness is similar to the X-ray one, and *(iii)* the monochromatic radio power at 1.4 GHz correlates strongly with the IC gas temperature. On the other hand, the same model predicts that radio halos should be present in every cluster, which is not actually observed, although the predicted radio halo luminosities can change by factors up to $\sim 10^2 \div 10^6$, depending on the amplitude and the structure of the intracluster magnetic field. Also, neutral pions arising from neutralino annihilation should give rise to substantial amounts of diffuse gamma-ray emission, up to energies of order M_χ,

that could be tested by the next generation gamma-ray experiments.

Subject headings: cosmology: general – Dark Matter: neutralino – galaxies: clusters: general – radio emission: general – radiation mechanisms: non-thermal.

1. Introduction

Dark Matter (DM) interaction and annihilation in the halo of our galaxy and in other galaxies have relevant astrophysical implications. In fact, if DM is constituted by weakly interacting massive particles (WIMP's), their annihilation can produce direct and indirect signals such as observable fluxes of positrons (Silk and Srednicki 1984, Rudaz and Stecker 1988, Ellis et al. 1989, Stecker and Tylka 1989, Kamionkowski and Turner 1991, Baltz and Edsjö 1998), antiprotons (Chardonnet et al. 1996, Bottino et al. 1998), gamma-rays (Bengtsson et al. 1990, Chardonnet et al. 1995) and neutrinos (Silk and Gondolo 1999) from the Milky Way halo.

Motivated by these results, we explore here some specific consequences of the production of positrons and electrons from the WIMP interaction in massive DM halos like clusters of galaxies. The decays of WIMP annihilation products (fermions, bosons, etc.) yield, among other particles, energetic electrons and positrons up to energies comparable to the WIMP mass (usually of the order of tens to hundreds GeV). It is straightforward to realize that these energetic electrons and positrons (hereafter we will refer to these particles as electrons because their distinction is not essential for our purposes) can emit synchrotron radiation in a DM halo which is filled with a magnetic field at the level of μG. Clusters of galaxies are the largest bound systems which have indeed both the largest amount of DM and extended Intra Cluster (IC) magnetic field at the level of a few μG. It is then natural to expect that the WIMP annihilation products can give origin to an extended radio emission.

Extended radio halos and relics are observed, at present, in more than 40 galaxy clusters (see, e.g., Owen et al. 1999, Feretti 1999, Giovannini 1999, Liang et al. 2000). Cluster radio halos show, generally, a regular morphology, which is similar to the X-ray morphology, a low surface brightness, and a steep radio spectrum, $J(\nu) \sim \nu^{-\alpha_r}$, with $\alpha_r \sim 1 \div 1.5$. The level of polarization in the radio halo emission is usually $\lesssim 10\%$ (Feretti

1999, Liang 2000). The radio halo sizes are typically of $(0.5 \div 1)h_{50}^{-1}$ Mpc, and are centered on the X-ray emission of the cluster. Their radio halo luminosity at 1.4 GHz, $J_{1.4}$, correlates strongly with the cluster IC gas temperature, T, and with its X-ray luminosity, L_X, mainly produced by thermal bremsstrahlung emission (see Colafrancesco 1999, 2000, Liang et al. 2000). This result points to a strong correlation between the physical state and origin of the relativistic electrons and the thermal content and distribution of the IC gas (see Colafrancesco 1999 , 2000 for a more extended discussion).

While we have a definite evidence for the existence of central radio halos in more than 20 rich clusters (see Section 6 below), the physical origin of such extended radio halos is still a matter of debate. The main difficulty in explaining the radio halo properties arises from the combination of their large size ($\sim$ 1 Mpc) and the short lifetimes ($\sim 10^8 - 10^9$ years) for synchrotron radiating electrons. Moreover, also the origin and the evolution of the IC magnetic field is still unclear (see, e.g., Kronberg 1994 for a review).

Successful models for the origin of non-thermal, diffuse radio emission from galaxy clusters have been proposed in the context of the possible cosmic ray acceleration mechanisms in the intra cluster medium (hereafter ICM). Synchrotron emission from a population of relativistic electrons (Jaffe 1977, Rephaeli 1977, Roland 1981) accelerated – or reaccelerated in situ (Schlikeiser 1987) – as primary cosmic rays (see Sarazin 1999 and references therein), or produced *in situ* as secondary products of *pp* collisions (Dennison 1980, Vestrand 1982; see also more recently Blasi and Colafrancesco 1999 and references therein) can reproduce the observed spectra of the radio halo emission from Coma (see Giovannini and Feretti 1996, Deiss et al. 1997 for an observational review). In all these models for the origin of radio halos, one needs a substantial energy supply to maintain the brightness of the radio halo for a time comparable with the Hubble time. The possibility that such energy budget can be supplied to a radio halo from shocks and turbulence induced

by strong cluster mergers (Sarazin 1999, Takizawa 2000) is suggested by the evidence that several radio halo clusters (e.g., A1656, A2255, A2163, A2319, A665) are undergoing a merger event. The shock waves produced by strong mergers could accelerate primary cosmic rays and amplify the IC magnetic field (see Roettiger 1999) to produce substantial radio powers. However, there are also some other clusters which still show extended radio halos (e.g., A2256, A2319, and other clusters found recently by Giovannini et al. 1999) but are either in a pre-merger state or even there is no clear merging event occurring. Moreover, there are also a few small-size radio halos found in clusters which have cooling flows (e.g., Perseus, A85, A2218 and maybe A2254). Therefore, one is bound to assume that: *i)* the energy released during the very early phases of the merging process is sufficient to power the central radio halo; or *ii)* the electrons are efficiently reaccelerated by the turbulent gas motion originated from IC turbulence and/or the galaxy motion within the cluster (Deiss et al. 1997); or *iii)* there exists a population of cosmic ray protons accelerated by galaxy activity and/or early cluster mergers which are stored for long times (see, Colafrancesco and Blasi 1998) in the cluster and produce *in situ* high-energy secondary electrons providing the long-living radio halos (Blasi and Colafrancesco 1999). So, while the energy needed for the maintenance of a radio halo can be reasonably accounted for, the origin of the seed relativistic electrons is not yet fully clear.

In this paper we explore the possibility that the diffuse radio halo emission observed in many clusters is produced by high-energy electrons resulting from the decay of the annihilation products of DM particles, like WIMP's. Among the WIMP's candidates, we consider in particular the lightest neutralino χ, that is predicted in supersymmetric extensions of the Standard Model (Haber and Kane 1985, Jungman et al. 1996). The χ mass is expected to be in the range of tens to hundreds GeV. The detailed interaction properties of the neutralino are determined once its physical composition is fixed. Indeed, neutralinos are a linear combinations of two Higgsinos (supersymmetric partners of the

Higgs bosons) and two gauginos (supersymmetric partners of the neutral gauge bosons). Both the neutralino mass and its physical composition affect in general the rate and the final state composition of the $\chi\chi$ annihilation process. Recent analysis of accelerator constraints, combined with cosmological DM requirements (Ellis et al. 2000), points to: *i*) a lightest neutralino heavier than about 46 GeV; *ii*) a lightest neutralino that is either a *pure* gaugino or a heavily mixed gaugino-Higgsino state, since a predominantly Higgsino state cannot provide a substantial component of the dark matter.

According to their physical composition and mass, neutralinos can annihilate either into fermion pairs or into vector (or Higgs) boson pairs. In general, for a pure-gaugino χ the annihilation into fermion pairs is dominant. Due to the chiral structure of the initial state, the annihilation cross section inside a halo grows with the square of the final fermion mass (see, e.g., Turner and Wilczek 1990), giving larger rates for heavier fermions. Hence, for pure gauginos, a continuum electron spectrum will arise both from the leptonic decays of b and c quarks and τ leptons, and from the decays of π's originating from the fragmentation of quark pairs. On the other hand, when the χ higgsino component is not negligible and $M_\chi > M_W$, the annihilation into WW (or ZZ) pairs can become dominant. In this case, the electron spectrum will arise partly from the leptonic direct W (or Z) decays (giving rise to energetic electron of energy $\sim M_\chi/2$), and partly from the hadronic vector boson decays, giving rise to electrons through both the leptonic heavy-quarks decays and π's decays.

In this paper, we bypass all the complicancies deriving from a detailed study of the supersymmetric parameter dependence of the neutralino annihilation cross sections, by adopting the following simplified framework, that will anyway reproduce the crucial features of the problem at hand:

a) we will assume a given value for the neutralino annihilation cross section, which is both relevant for the DM closure density and inside the allowed range of the supersymmetric

neutralino cross sections for a given M_χ and neutralino composition. A different value of the cross section can then be straightforwardly rescaled from our results, as we will discuss in the paper;

b) we will study the electron energy spectrum arising from the decays of the neutralino annihilation products in the two distinct situations where the dominant annihilation is either into fermions or into vector bosons. A realistic case will be, of course, close to either these two or to a linear combination of them.

This simplified scheme will be representative of a wide range of supersymmetric models that are relevant for the DM problem.

The plan of the paper is the following. In Section 2 we discuss the annihilation process of neutralinos in the DM halos of galaxy clusters, and in Section 3 we give an analytical approximation for the source spectrum of high-energy electrons produced from the decay of the secondary products of $\chi\chi$ annihilation. In this Section we also derive the electron equilibrium spectrum. In Section 4 we evaluate the radio halo spectrum and its brightness profile from synchrotron emission of the relativistic $e^{\pm}$ and the level of ICS emission from the same population of electrons. In Section 5 we discuss the specific cases of the radio halos found in Coma and in the cluster 1E0657-56 and in Section 6 we show how the present model is able to reproduce the $J_{1.4} - T$ relation. We summarize the results of this paper and discuss the relevance of the present model for the origin of cluster radio halos in Section 7. The relevant physical quantities are calculated using $H_0 = 50$ km s^{-1} Mpc^{-1} and a flat($\Omega_0 = 1$) CDM dominated cosmological model.

2. Neutralino annihilation in galaxy clusters

Neutralinos decouple from the primeval plasma when they are no longer relativistic. Their present abundance can be calculated by solving the Boltzmann equation for the evolution of the density of particle species (see, e.g., Kolb and Turner 1990).

Assuming a spherical, uniform top-hat model for the collapse of a cluster (see, e.g., Peebles 1980), the average DM density within a halo which virializes at redshift z is:

$$\bar{\rho} = \Delta(\Omega_0, z)\rho_b\Big(1 - f_g\Big) \tag{1}$$

where the background density is $\rho_b = \Omega_m \rho_c$ and $\Delta(\Omega_0, z)$ is the non-linear density contrast of the virialized halo (see, e.g., Colafrancesco et al. 1997). Here f_g is the gas mass fraction. If we redistribute the total mass, $M = \frac{4\pi}{3}\bar{\rho}R_p^3$, found within the radius $R_p = pr_c$ (expressed in terms of the cluster core radius r_c), according to a density profile $\rho(r) = \rho_0 g(r)$, we find that the central total density is given by:

$$\rho_0 = \frac{\bar{\rho}}{3}\frac{R_p^3}{I(R_p)} \ , \tag{2}$$

where $I(R_p) = \int_0^{R_p} dr r^2 g(r)$. In our phenomenological approach, we consider two cases: a constant core model and a central cusp profile.

The constant core model with a density profile:

$$g(r) = \left[1 + \left(\frac{r}{r_c}\right)^2\right]^{-\xi/2} \ , \tag{3}$$

assumed here to be given from a beta-profile (Cavaliere and Fusco-Femiano 1976) with $\xi = 3\beta$ and $\beta = \mu m_p v^2/kT$, gives:

$$\rho_0 = \frac{\bar{\rho}}{3}\frac{p^3}{I(p,\beta)} \tag{4}$$

with $p \equiv R_p/r_c$ and $I(p,\beta) = \int_0^p dx x^2(1+x^2)^{-3\beta/2}$ (here $x \equiv r/r_c$ in terms of the cluster core radius r_c).

The central cusp model described by a profile:

$$g(r) = \left(\frac{r}{r_c}\right)^{-\eta}\left(1+\frac{r}{r_c}\right)^{\eta-\xi} \tag{5}$$

gives:

$$\rho_0 = \frac{\bar{\rho}}{3}\frac{p^3}{I(p,\eta,\xi)} \ , \tag{6}$$

where $I(p,\eta,\xi) = \int_0^p dx x^{2-\eta}(1+x)^{\eta-\xi}$. With $\eta = 1$ and $\xi = 3$, the central cusp model corresponds to the "universal density profile" which Navarro, Frenk and White (1997; hereafter NFW) showed to be a good description of cluster DM halos in N-body simulations of CDM hierarchical clustering. Note that, in both models the DM density scales, at large radii, as $r^{-\xi}$.

Assuming that the DM density scales like the total cluster density, a general expression for the central DM number density is:

$$n_{\chi,0} = \frac{\bar{n}}{3}\frac{p^3}{I} \tag{7}$$

where the integral I is given in eqs. (4) or (6) for the two DM profiles here considered, and

$$\bar{n} = 4.21 \cdot 10^{-5} \text{ cm}^{-3} \ \Omega_\chi h^2 \Big[\frac{M_\chi}{100 \ GeV}\Big]^{-1}\Big[\frac{\Delta(\Omega_0,z)}{400}\Big](1-f_g) \ . \tag{8}$$

Here we assume that most of the DM consists of neutralinos of mass M_χ.

The annihilation rate of neutralinos in a DM halo is

$$R = n_\chi(r)\langle\sigma V\rangle_A \ , \tag{9}$$

where $n_\chi(r) = n_{\chi,0}g(r)$ is the neutralino number density and $\langle\sigma V\rangle_A$ is the $\chi\chi$ annihilation cross section averaged over a thermal velocity distribution at freeze-out temperature. Although, as anticipated, the $\chi\chi$ annihilation cross section is a nontrivial function of the

mass and physical composition of the neutralino, to our purpose it suffices to recall that the χrelic density is approximately given by (Jungman et al. 1996):

$$\Omega_\chi h^2 \simeq \frac{3 \times 10^{-27}\ \mathrm{cm}^3\ \mathrm{s}^{-1}}{\langle \sigma V \rangle_A} \quad . \tag{10}$$

Hence, for the $\chi\chi$ annihilation, we will assume a total χ cross section of

$$\langle \sigma V \rangle_A \approx 10^{-26}\ \mathrm{cm}^3\ \mathrm{s}^{-1} \tag{11}$$

to be consistent with the value $\Omega_m \sim 0.3$ derived from clusters of galaxies and large scale structure constraints (see, e.g., Bahcall 1999). Detailed studies of the relic neutralino annihilation (Edsjö 1997) show that the above value is well inside the allowed range predicted in supersymmetric theories for a wide choice of masses and physical compositions of neutralinos that can be relevant as cold DM candidates. Enhancing the χ annihilation rate will have on our results the simple effect of rescaling the final electron spectra by the same enhancement factor

For values of h in the range $0.5 \lesssim h \lesssim 1$, we can infer that for a flat, vacuum dominated CDM universe with Ω_Λ in the range $0.5 \div 0.7$ and $\Omega_\chi \sim 0.3 \div 0.5$, the quantity $\Omega_\chi h^2$ takes values in the range $\sim 0.075 \div 0.5$, which would fix the annihilation cross section to within a factor less than ten.

3. Production and equilibrium electron spectra

3.1. The source spectrum

Neutralinos which annihilate in a DM halo produce quarks, leptons, vector bosons and Higgs bosons, depending on their mass and physical composition (see, e.g., Edsjö 1997). Following the discussion in Section 1, monochromatic electrons (with energy about M_χ), coming from the direct channel $\chi\chi \to ee$, are in general much suppressed (Turner and

Wilczek 1990). Electrons are then produced from the decay of the final heavy fermions and bosons.

The different composition of the $\chi\chi$ annihilation final state will in general affect the form of the final electron spectrum. To our purpose, it will be sufficient to consider two somewhat extreme cases: 1) a pure-gaugino annihilation, which yields mainly fermion pair direct production $\chi\chi \to ff$, with cross sections scaling as M_f^2 for different fermions (Turner and Wilczek 1990); 2) a mixed gaugino-higgsino state in the case of a dominant annihilation into W (and Z) vector bosons, $\chi\chi \to WW(ZZ)$. A real situation will be mostly reproduced by either of the above two cases, or by a linear combination of the two.

The positron spectrum arising from the $\chi\chi$ annihilation has been derived by various authors (Silk and Srednicki 1984, Rudaz and Stecker 1988, Ellis et al. 1989, Stecker and Tylka 1989, Turner and Wilczek 1990, Kamionkowski and Turner 1991, Baltz and Edsjö 1998). Here, we will adopt the approaches by Rudaz and Stecker (1988; hereafter RS) and by Kamionkowski and Turner (1991; hereafter KT), that gave the analytical approximations of the positron source functions for models in which neutralinos annihilate mainly into fermions and vector bosons, respectively. Here we report the results of our calculations while the details of these two approaches are presented in the Appendix.

The total source spectra in the two cases considered are shown in Fig.1 for $M_\chi = 100$GeV. The heavy solid curve is the total spectrum for the model in which fermions dominate the annihilation. We also show the different contributions to the total source spectra from fermions, i.e. the source spectrum for first-generation prompt electrons (P1), second-generation prompt electrons (P2) and secondary electrons produced in the decay of charged pions (π). The total source spectrum is rather smooth and, when approximated by a single power-law, it has an overall slope $Q_e \sim E^{-1.9}$ in the interesting energy range $0.02 \leq E/M_\chi \leq 0.7$.

The source spectra for the model in which gauge bosons dominate the annihilation is given by the light solid curve. For this case we show the contributions from the decay $W^{\pm} \to \tau^{\pm} \to e^{\pm}$; $W^{\pm} \to c \to e^{\pm}$ (labelled as KT_1) and from the decays of charged pions produced in hadronic decays of the $W^{\pm}$ (labelled with KT_π). Note that we make this analysis restricting only to the WW channel, since the ZZ contribution gives rise to a qualitatively similar spectrum.

Two prominent spectral features (bumps) around $E \sim M_\chi/2$ (arising from the direct decay $W \to e\nu$) and $E \sim M_\chi/20$ are shown by the model in which gauge bosons dominate the annihilation, in comparison with the smoother spectral shape of the fermion dominated annihilation. These spectral features are more prominent in Fig.2 where we plot the quantity $E^3 Q_e(E, r)$. From a closer inspection of Figs.1 and 2, one can see that the main difference between the two models stands in the height and width of the bumps at energies below $M_\chi/10$, where the pion-produced electrons dominate the source spectrum, and in the high-energy tail at $E \lesssim 0.7 M_\chi$ where the P1 contribution dominates. In both models, electrons produced by tertiary decays of gauge bosons are neglected because their contribution is subdominant with respect to the pion decay distribution.

In the calculation of the radio halo emission (see Section 4 below) the source spectra of eq.(A1) and A(18) will be multiplied by a factor 2 to take into account the contribution of both electrons and positrons.

3.2. The electron equilibrium spectrum

The time evolution of the electron spectrum is given by the transport equation:

$$\frac{\partial n_e(E,r)}{\partial t} - \frac{\partial}{\partial E}\Big[n_e(E,r) b(E)\Big] = Q_e(E,r) \tag{12}$$

where $n_e(E,r)$ is the equilibrium spectrum at distance r from the cluster center for the electrons with energy E. The source electron spectrum rapidly reaches its equilibrium configuration mainly due to synchrotron and Inverse Compton Scattering (hereafter ICS) losses at energies $E \gtrsim 150$ MeV and to Coulomb losses at smaller energies (Blasi and Colafrancesco 1999). Since these energy losses are efficient in the ICM and DM annihilation continuously refills the electron spectrum, the population of high-energy electrons can be described by a stationary transport equation ($\partial n_e/\partial t \approx 0$)

$$-\frac{\partial}{\partial E}\Big[n_e(E,r)b(E)\Big] = Q_e(E,r) \tag{13}$$

from which the equilibrium spectrum can be calculated. Here, the function $b(E)$ gives the energy loss per unit time at energy E

$$b_e(E) = \left(\frac{dE}{dt}\right)_{ICS} + \left(\frac{dE}{dt}\right)_{syn} + \left(\frac{dE}{dt}\right)_{Coul} = b_0(B_\mu)E^2 + b_{Coul}\ , \tag{14}$$

where $b_0(B_\mu) = (2.5\cdot 10^{-17} + 2.54\cdot 10^{-18}B_\mu^2)$ and $b_{Coul} = 7\times 10^{-16}n(r)$ (if b_e is given in units of GeV/s). In the expression for b_{Coul}, the IC gas density, $n(r)$, is given in units of cm^{-3}.

The equilibrium spectrum calculated combining the source spectrum $Q_e(E,r)$ and the energy losses $b(E)$ is shown in Fig.3 for the two cases here considered. Equilibrium spectra are evaluated separately for the different components of the source spectra and then summed together. This spectrum is evaluated within the cluster core for a constant core density (see eq.2) with a reference value of the central density $n_{\chi,0} = 1\ cm^{-3}$ and $\langle\sigma V\rangle_A = 10^{-26}$ cm^3 s^{-1}. This equilibrium spectrum can be easily calculated for other cluster configurations by scaling the parameters of the cluster density profile. The equilibrium spectrum for the case in which neutralino annihilation is dominated by fermions, is smooth enough that it can be reasonably approximated by a power-law, $n_e(E) \sim E^{-p}$, down to $E \sim M_\chi/30$ with a slope $p \sim 2.9$. We will make use of this convenient approximation in the discussion of our results.

3.3. Comparison between approximated and Monte Carlo results

The source spectra in Fig. 1 arise from an analytic approximation (see the Appendix) of the exact shape of the electron spectrum that tries to cope with the details of the quarks and leptons decays and of the hadronization of the decay products. Detailed $e^{\pm}$ spectra can also be obtained by using state-of-the-art Monte Carlo simulations, although the analytical approximations used here are able to recover the relevant aspects of more detailed studies.

There are, however, some differences among the equilibrium spectra obtained from different studies using Monte Carlo techniques. We can compare here our analytical approximations with the results of the Monte Carlo simulations run by Baltz and Edsjö (1998), and Golubkov and Koplinoch (1998). Note that the latter study considers massive neutrinos annihilation, that, as far as the electron spectra shapes are concerned, should be equivalent to the neutralino annihilation at fixed $M_\chi = m_\nu$, and fixed ff/WW annihilation dominance. One can note that for the case we consider here, i.e. $M_\chi = 100$ GeV, the total equilibrium electron spectrum from the simulations of Golubkov and Konoplich (1998) agrees quite well with the spectrum shown in Fig.3 for the case in which neutralinos annihilate mainly into fermions. On the other hand, the case in which the annihilation is dominated by vector bosons (KT) is quite well reproduced by the simulations in Baltz and Edsjö (1998), although there a slightly different value of M_χ (i.e., $M_\chi \sim 130$ GeV) is assumed.

However, beyond the limits of the present discussion, it is worth noticing that there are still differences in the electron spectra so far published by different authors using Monte Carlo techniques. In view of this, we conservatively assume in our calculations a reasonable uncertainty of a factor ~ 2 in the amplitude of the electron spectrum, and of $\sim 10\%$ in its slope. We will consider more detailed predictions derived from available Monte Carlo simulations in a forthcoming paper.

4. The diffuse radio halo emission

The calculation of the radio emissivity per unit volume is performed here in the simplified assumption that electrons with energy E radiate at a fixed frequency given by :

$$\nu \approx 3.7 \text{ MHz } B_\mu \Big(\frac{E}{\text{GeV}}\Big)^2 \ . \tag{15}$$

This approximation introduces negligible errors in the final result and has the advantage of making it of immediate physical interpretation.

The radio emissivity at frequency ν and at distance r from the cluster center can be calculated as

$$j(\nu, r) = n_e(E, r) \left(\frac{dE}{dt}\right)_{syn} \frac{dE}{d\nu} \ , \tag{16}$$

where $(dE/dt)_{syn}$ is given in eq.(14). The radio halo luminosity is obtained by integration of $j(\nu, r)$ over the cluster volume yielding:

$$J(\nu) = 4\pi \int_0^{R_{halo}} dr \ r^2 j(\nu, r) \ , \tag{17}$$

where R_{halo} is the size of the cluster radio halo. The observed radio halo flux is then

$$F(\nu) = \frac{J(\nu)}{4\pi D_L^2}$$

where $D_L(z, \Omega_0)$ is the cluster luminosity distance (see, e.g., Weinberg 1972). For the sake of illustration, we give the explicit form of $J(\nu)$ in the case of a power-law source spectrum, $Q(E, r) = Q_0 (E/E_0)^{-s}$, where $Q_0 = n_\chi^2(r) \langle \sigma V \rangle_A (k M_\chi)^{-1}$ and E_0 is a normalization energy, say 1 GeV. Using eqs. (13), (16) and (17), we can write

$$J(\nu) = \frac{4\pi n_{\chi,0}^2 \langle \sigma V \rangle_A (k M_\chi)^{-1}}{2(s-1)} \Big(\frac{E_*}{E_0}\Big)^{-s+2} E_0 \mathcal{I} \frac{b_{0,syn}(B_\mu)}{b_0(B_\mu)} B_\mu^{\alpha_r - 1} \nu^{-\alpha_r} \tag{18}$$

where $\alpha_r = s/2$, $E_* = 16.44$ GeV, $\mathcal{I} = \int_0^{R_{halo}} dr r^2 g^2(r)$, $b_0(B_\mu) = (2.5 \cdot 10^{-17} + 2.54 \cdot 10^{-18} B_\mu^2$ and $b_{0,syn}(B_\mu) = 2.54 \cdot 10^{-18} B_\mu^2$. For $B_\mu \lesssim 3.14$, the radio luminosity scales in eq.(18) as $J(\nu) \propto n_{\chi,0}^2 \langle \sigma V \rangle_A (k M_\chi)^{-1} B_\mu^{\alpha_r + 1} \nu^{-\alpha_r}$.

In the calculation of the radio halo luminosity we consider both the case of a uniform IC magnetic field and a case in which the magnetic field has a radial profile which declines with the distance from the cluster center, as indicated by recent numerical simulations (see, e.g., Friaca and Goncalves 1998). Specifically, we considered a magnetic field density profile

$$B = B_0\Big[1 + \Big(\frac{r}{r_{c,B}}\Big)^2\Big]^{-w/2} \tag{19}$$

with values $w \sim 0.5 \div 1$. Here, for simplicity, we assume that the spatial structure of the magnetic field is given by a constant core profile with lenght scale $r_{c,B}$.

4.1. The radio halo spectrum and spatial distribution

The total radio halo flux predicted from our model has generally a steep spectrum with average slope $\alpha_r \sim 1.2 - 1.8$, depending on the neutralino mass and composition and on the shape of the DM density and magnetic field profiles. We will discuss more specifically this point in Section 5 below. Here we want to emphasize that for a fixed value of the magnetic field B, the neutralino mass fixes the maximum frequency at which we can observe synchrotron emission from the radio halo,

$$\nu_{max} \sim 3.7 \text{ MHz } B_\mu\Big(\frac{kM_\chi}{GeV}\Big)^2 \tag{20}$$

For $M_\chi = 100$ GeV and $k \approx 0.7$ (see Appendix), the maximum frequency at which the radio halo spectrum is observable is $\nu_{max} \approx 18.1$ GHz $\times B_\mu$. From this fact, we can use the available data on the radio halos of Coma and 1E0657-56 (see Figures 3 and 4) to set a lower limit to the neutralino mass. Specifically, the maximum frequency, $\nu_{max,obs}$, at which the radio halo spectrum is observed sets a lower limit

$$M_\chi \geq \frac{16.44}{k} \text{ GeV } \Big(\frac{\nu_{max,obs}}{\text{GHz}}\Big)^{1/2} B_\mu^{-1/2} \tag{21}$$

which gives $M_\chi \geq 74.3$ GeV $B_\mu^{-1/2}$, for $\nu_{max,obs} = 10$ GHz. Furthermore, the present theory predicts a sharp cutoff in the radio halo spectrum at ν_{max} given by eq.(20); so,

high frequency observations can both test the neutralino model and measure the quantity $B_\mu(kM_\chi)^2$ from the possible detection of the high-ν sharp cutoff in the radio halo spectrum.

The brightness profile of the radio halo is obtained by integration of the emissivity, $j(\nu, r)$, along the line of sight. It scales, for a power-law radio halo spectrum, as

$$S_{radio} \propto \int d\ell \; n^2(r) \cdot B^{1+\alpha_r}(r) \tag{22}$$

and declines at large radii as $r^{-[\xi+w(1+\alpha_r)]+1/2}$. The radio halo brightness profile resembles, for both the DM profiles here considered, the X-ray brightness profile of the cluster which scales as

$$S_{X-ray} \propto \int d\ell \; n^2(r) \cdot T^{1/2}(r) \; . \tag{23}$$

In particular, for a uniform magnetic field, $B = \text{const}$, and for a isothermal cluster, $T = \text{const.}$, the brightness S_{radio} behaves exactly as the X-ray brightness S_{X-ray} at all radii. Small deviations from this behaviour can be attributed to radial variations in $B(r)$ and/or in $T(r)$.

The radio halo brightness profile depends on the assumed DM profile (see eqs.19 and 22). Specifically, at small radii the constant core model still gives a radio brightness profile that resembles the X-ray emission profile while the central cusp model tends to give a radio brightness which is more peaked toward the center. Thus, the model predicts a strong radio emissivity at the cluster center under the assumption of a central cusp (or NFW) profile. However, neutralino annihilation can also cause a softening of the central DM cusp due to the high interaction rate of neutralinos in the central region of the clusters with respect to the outer parts (see Kaplinghat, Knox and Turner 2000). This countereffect weakens the aforementioned problem.

4.2. Inverse Compton Scattering emission

The relativistic electrons which are responsible for the radio halo emission also emit X-rays and UV photons through Inverse Compton Scattering (ICS) off the Cosmic Microwave Background photons. As in the case of the synchrotron emission, also for ICS we can adopt the approximation that electrons radiate at a single energy, given by

$$E_X = 2.7\ keV\ E^2(GeV). \tag{24}$$

Electrons with energy in excess of a few GeV radiate in the hard X-ray range, while electrons with energy smaller than ~ 400 MeV produce soft X-rays and UV photons. The non-thermal X-ray/UV emissivity at distance r from the cluster center is evaluated as

$$\phi_X(E_X, r) = n_e(E, r) \left(\frac{dE}{dt}\right)_{ICS} \frac{dE}{dE_X}\ . \tag{25}$$

In complete analogy with the case of the radio emission, the integrated non-thermal X-ray luminosity, $\Phi_X(E_X)$ is

$$\Phi(E_X, r) = \int_0^{R_{halo}} dr\ 4\pi r^2 \phi_X(E_X, r)\ . \tag{26}$$

The predicted X-ray fluxes from ICS emission due to the electrons produced in $\chi\chi$ annihilation are lower than those required to explain the hard X-ray excesses currently observed in Coma, A2256 and A2199, and do not contribute substantially to the EUV and hard X-ray emission excesses of these clusters.

5. Application to observed radio-halo clusters: Coma and 1E0657-56

Our theory for the origin of radio halos in clusters can reproduce successfully the spectra of the radio halo emission observed from Coma (Giovannini et al. 1993, Deiss et al. 1997) and 1E0657-56 (Liang et al. 2000). Moreover, these data in turn can set interesting constraints to the mass and composition of the neutralino.

For any cluster, we choose a DM central density, $n_{\chi,0}$, which is given by eq. (7) evaluated with the parameters appropriate to each cluster and, in the case of 1E0657-56, with parameters approriate to each reagion in which the radio halo spectrum has been observed.

In the case of Coma we choose the following parameters: $r_c = 0.4 h_{50}^{-1}$ Mpc, $\beta = 0.76$, $n_{\chi,0} = 3 \cdot 10^{-3}$ cm^{-3}. The radio halo spectrum has been integrated out to a radius $R_{halo} = 1.3 h_{50}^{-1}$ Mpc (see, e.g., Giovannini et al. 1993). In the model in which neutralino annihilation is dominated by fermions ($\chi\chi \rightarrow ff$), a uniform magnetic field $B_{uniform} \approx 1.3$ μG is needed to fit the spectrum under the assumption of a constant core profile. In the case of a declining magnetic field $B = B_0[1+(r/r_{c,B})^2]^{-0.7}$, a value $B_0 = 8$ μG fits better the data, under the same model assumptions. The resulting spectra are shown in Fig.4. In this figure we also show the spectra derived from the power-law approximation of the equilibrium spectrum shown in Fig.3. A radially decreasing magnetic field yields a slightly steeper spectral slope, as it should be expected from eq.(17).

Under the same assumptions of a constant core profile and radially decreasing magnetic field, the model in which neutralino annihilation is dominated by gauge bosons ($\chi\chi \rightarrow WW$) does not fit the Coma radio halo (see Fig.4). Within the limits of the analytical approximations used in this paper, the Coma data exclude this model at more than 3 standard deviations (see Fig.5). In this figure we also show the range of uncertainties in the final radio halo spectra calculated considering an uncertainty of a factor ± 2 in the overall normalization of the source spectra and $\pm 10\%$ uncertainty on their slopes, for the two extreme annihilation model here considered.

In the case of the distant cluster 1E0657-56 at $z = 0.269$, we choose different parameters according to the two different regions in which the spectrum has beem measured (we use the core radii and β parameters given in Liang et al. 2000). We assume that neutralino

annihilation is dominated by fermions ($\chi\chi \to ff$) and consider a constant core DM density profile. For the outer region we choose $r_c = 0.38 h_{50}^{-1}$ Mpc, $\beta = 0.7$, $n_{\chi,0} = 9 \cdot 10^{-3}$ cm^{-3}. The radio halo spectrum has been integrated out to a radius $R_{halo} = 2 h_{50}^{-1}$ Mpc (Liang et al. 2000). A uniform magnetic field $B_{uniform} \approx 2.$ μG is needed to fit the spectrum of the outer region. In the case of a declining magnetic field $B = B_0[1 + (r/r_{c,B})^2]^{-0.5}$, a value $B_0 = 100$ μG can fit the data. For the inner region we choose $r_c = 0.08 h_{50}^{-1}$ Mpc, $\beta = 0.49$ and the same central density $n_{\chi,0} = 9 \cdot 10^{-3}$ cm^{-3}. The radio halo spectrum has been integrated out to a radius $R_{halo} = 0.6 h_{50}^{-1}$ Mpc. A uniform magnetic field $B \approx 9$ μG is needed to fit the spectrum of this region. In the case of a declining magnetic field $B = B_0[1 + (r/r_{c,B})^2]^{-0.5}$, a value $B_0 = 100$ μG fits the data. The results are shown in Fig.7. As in the case of Coma, the extreme case of neutralino annihilation dominated by gauge bosons ($\chi\chi \to WW$) is inconsistent with the radio halo spectrum of this cluster.

Note that the radio-halo spectra shown in Figures 4-7 are calculated assuming a constant core density profile for the DM component. A central cusp model gives a higher central density and increases the χ annihilation rate in the central region of the cluster which in turn produces more high-energy electrons per unit volume. This increase in the electron density must be compensated by a decrease in the magnetic field value needed to fit the radio halo spectrum. In fact, assuming a NFW density profile for Coma, a uniform magnetic field $B_{uniform} = 0.45 \mu$G is required to fit the data. Alternatively, a central value of the magnetic field, $B_0 = 1.4 \mu$G is able to fit the spectrum assuming a B radial profile as given by eq. (19). We show the difference between the spectra obtained either with a beta-profile or with a NFW profile in Figure 8.

6. The $J_{1.4} - T$ relation for radio-halo clusters

Another interesting property of radio halo clusters is the steep correlation existing between the monochromatic radio halo luminosity observed at 1.4 GHz, $J_{1.4}$, and the IC gas temperature: $J_{1.4} \sim T^q$ with $q = 6.25$ (range $q = 4.1 \div 12.5$ at 90% confidence level) found by Colafrancesco (1999, 2000) and confirmed by Liang et al. (2000). Radio luminosity data are taken from Feretti (1999), Giovannini et al. (1999), Liang et al. (1999) and Owen et al. (1999). Here, we use the temperature data from Arnaud and Evrard (1999), bur a similar result obtains using temperature data from Wu, Xue and Fang (1999) or David et al. (1993). Such a steep correlation (see Fig.9) can be reproduced in models of radio halos powered by acceleration of cosmic rays triggered either by strong merging events or by enhanced galaxy activity, but requires specific conditions for the structure of the magnetic field (see Colafrancesco 1999, 2000 for a discussion).

In the model we present here the radio halo luminosity (see eqs.17-18) scales as

$$J(\nu) \propto n_{\chi,0}^2 r_c^3 \langle \sigma V \rangle_A B^{1+\alpha_r} \nu^{-\alpha_r} \tag{27}$$

where $\alpha_r = dlnJ(\nu)/dln\nu$ is the effective slope of the radio halo spectrum. Thus, the monochromatic radio halo luminosity correlates naturally with the cluster X-ray bremsstrahlung luminosity, $L_X \propto n_0^2 f_g^2 r_c^3 T^{1/2}$ (here n_0 is the central IC gas density and $f_g = M_{gas}/M$ is the cluster baryon fraction), to give

$$J_{1.4} \propto L_X f_g^{-2} T^{-1/2} \langle \sigma V \rangle_A B^{1+\alpha_r} \ . \tag{28}$$

Using the observed correlation, $L_X \sim T^b$ with $b \sim 3$ (see, e.g., Arnaud and Evrard 1999, Wu et al. 1999, David et al. 1993) and assuming that $f_g = const$, as indicated by the available cluster data (Jones and Forman 1999, Mohr 2000), we derive

$$J_{1.4} \sim T^{(4b-1)/2} \langle \sigma V \rangle_A B^{1+\alpha_r} \tag{29}$$

Under the condition – assumed in this paper – of hydrostatic equilibrium of the cluster material with the overall potential wells, the relation $V \sim T^{1/2}$ holds, and we finally obtain:

$$J_{1.4} \sim T^b B^{1+\alpha_r} \ . \tag{30}$$

If every cluster has the same value of the magnetic field (universality condition), a correlation $J_{1.4} \sim T^3$ obtains. This is too flat compared to the observed correlation. However, the universality condition $B = \text{const}$ is rather unlikely. In fact, we expect that B increases with increasing T either under the condition of energy equipartition between the IC gas and the magnetic field (which yields $B \sim T^{1/2}$) or even under the condition of a B field which is frozen-in the ICM (i.e., $B \sim n^\gamma$ with $\gamma \sim 2/3$, which yields $B \sim T^{(b-2)\gamma}$).

In conclusion, it is reasonable to expect a quite steep correlation, $J_{1.4} \sim T^{4.15\pm0.25}$ or $J_{1.4} \sim T^{4.40\pm0.26}$, for an equipartition or frozen-in magnetic field. Such a correlation is consistent (within the uncertainties) with the best fit result given above and can reproduce the overall distribution of clusters in the $J_{1.4}-T$ plane. Moreover, since $T \propto (1+z)\Delta^{1/3}(\Omega_0, z)$ in CDM models of structure formation (see, e.g., Colafrancesco et al. 1997), the radio halo power is expected to evolve strongly with redshift $J_{1.4} \sim [(1+z)\Delta^{1/3}(\Omega_0, z)]^q$. Thus, already at $z \sim 0.2$ its normalization increases by a factor ~ 2 (we use here $q = 4$ as a reference value). The $J_{1.4} - T$ correlation predicted in the present model at $z = 0$ and at $z = 0.25$ is shown in Fig.9. The large steepness $q \approx 6.25$ deduced by a formal power-law fit to the data can be due to a superposition of the different correlations of radio halo clusters observed in the range $z \approx 0 \div 0.3$.

7. Discussion and conclusions

In this paper we have shown that the basic properties (i.e., the spectrum, the surface brightness profile and the $J_{1.4} - T$ correlation) of radio halos in galaxy clusters

can be reasonably fitted by a model in which the high-energy electrons, giving rise to the synchrotron emission, arise from the decay of secondary products of the neutralino annihilation in the DM halos of galaxy clusters. The slope and the frequency extension of the spectrum can set interesting constraints on the neutralino mass and composition. In fact, the highest observed frequency of the radio halo spectrum set a lower limit to the neutralino mass:

$$M_\chi \geq 16.44 \text{ GeV } k^{-1}\Big[\Big(\frac{\nu_{max,obs}}{GHz}\Big)\frac{1}{B_\mu}\Big]^{1/2} .$$

In particular, the highest frequency ($\nu \sim 4.85$ GHz) at which the Coma spectrum has been observed requires $M_\chi \geq 54.6$ GeV $B_\mu^{-1/2}$. A more stringent limit, $M_\chi \geq 70.5$ GeV $B_\mu^{-1/2}$, is obtained from the cluster 1E0657-56. Radio halo observations at frequencies larger than $5 \div 10$ GHz are not yet available, but are important to test the present model. In fact, the detection of a high frequency cutoff, ν_{cut}, in the radio halo spectra gives an upper limit on the neutralino mass. The high-ν cutoff predicted in our model, has the same value, $\nu_{cut} = 3.7$ MHz$B_\mu[k(M_\chi/GeV)]^2$, for all radio halos and depends only on the neutralino mass and the IC magnetic field. For a fixed neutralino mass and composition, the observations of this high-ν cutoff can yield a direct estimate of the cluster magnetic field.

In the same framework, the slope of the radio halo spectrum gives an indication on the neutralino physical composition. The radio halo spectrum of the two clusters considered here are well fitted by a model in which the neutralinos behave like pure gauginos, and annihilate mainly into fermions. On the other hand, when the neutralino annihilation is dominated by vector bosons (implying a non-negligible higgsino component), the electron source spectrum is too steep and shows two unobserved bumps at low and high energies (see Figs.1 and 2). This feature is also evident in the final radio halo spectrum (see Fig.5). Indeed, Figs. 5 and 6 show how far the neutralino model dominated by vector bosons is from reproducing the data of the radio halo spectrum of Coma and 1E0657-56.

After setting the neutralino mass and composition, the slope of the radio halo spectrum still depends on the DM density profile and on the magnetic-field radial profile, that influence the annihilation rate and the synchrotron emission power, respectively. The available data on Coma indicate (in the case of a constant core density profile) that a radially decreasing magnetic field is favoured to fit the correct steepness of the spectrum at high frequencies. This constraint is tighter for Coma, where an upper limit of 52 mJy at $\nu = 4.85$ GHz has been measured (see, e.g., Deiss et al. 1997), than for 1E0657-56, where a rather constant slope is observed up to $\nu \sim 10$ GHz. For a constant core density profile, the spectra of Coma and 1E0657-56 are consistent either with uniform IC magnetic fields $B_{uniform} \sim 1.3 \div 2\ \mu G$ or central values $B_0 \sim 8 \div 100\ \mu$G for a magnetic field profile $B(r) \sim r^{-1}$ at large distances from the cluster center. Using a central cusp (NFW) density profile increases slightly the slopes of the radio halo spectrum, reducing consequently the need for a magnetic field strongly decreasing with the distance from the cluster center. The central cusp profile requires also IC magnetic field amplitudes lower by a factor $\sim 3 \div 5$ to fit the radio halo spectrum.

The present model also predicts a mild steepening of the radio halo spectrum with increasing distance from the cluster center. This effect is mainly due both to the lower DM densities (which decrease the neutralino annihilation rate) and to a decrease of the IC magnetic field (which reduces the emitted powers via synchrotron emission) at large distances from the cluster center. The model presented here can fit reasonably well the radio halo spectra of the cluster 1E0657-56 in the inner and outer regions at which it has been measured by Liang et al. (2000). It also gives values for the radio spectral index of Coma $\alpha_r \sim 0.9 \div 1.6$, from the cluster center out to ~ 1 Mpc. These values are consistent (within the given uncertainties) with the increase of the radio spectral index of Coma given by Giovannini et al. (1993).

It is also noticeable that the spatial extension of the radio halo emission which is predicted in the present model is very similar to that of the X-ray emission from the IC gas, a property which has been emphasized in several observational works (see, e.g., Feretti 1999, Liang et al. 2000). Changes of radio halo/X-ray surface brightness ratio, S_{radio}/S_{X-ray}, with radius can be accounted for by radial variations of the IC magnetic field and/or the IC gas temperature.

The analysis presented in this paper is made for a value of the neutralino annihilation cross-sections $\langle\sigma V\rangle_A \approx 10^{-26}\ cm^3 s^{-1}$. This value is well inside the allowed range for a neutralino relevant as a DM candidate, and can be rescaled in a straightforward way from our results, for different assumptions on $\langle\sigma V\rangle_A$. Because the radio halo spectrum power (see eqs.17-18) scales linearly with $\langle\sigma V\rangle_A n_\chi^2 B^{1+\alpha_r}$ (here $\alpha_r = dlnF(\nu)/dln\nu$ is the effective spectral slope), higher (lower) values of the annihilation cross section imply lower (higher) DM densities, and require a lower (higher) IC magnetic field.

Another interesting aspect of the present model for the origin of cluster radio halos is that it can reproduce fairly well the observed correlation between the monochromatic radio halo power, $J_{1.4}$, and the IC gas temperature T. The steep $J_{1.4} - T$ relation shown by the available radio-halo clusters can be reproduced in our model as a superposition of evolutionary effects of the correlation $J_{1.4} \sim T^q$, with $q \sim 4.2 \div 4.4$, which results from the dependence of the electron spectrum, $n_e(E, r) \propto n_\chi^2(r)\langle\sigma V\rangle_A$, from the DM density, $n_\chi(r)$, and annihilation cross-section, $\langle\sigma V\rangle_A$, with the further assumption of an energy equipartition between the IC gas and the IC magnetic field.

The ICS emission from the same population of relativistic electrons produces unavoidably also fluxes of UV and X-ray emission that, however, are not so intense to reproduce the emission excesses in the EUV (Lieu et al. 1996) and in the hard X-rays (Fusco-Femiano et al. 1999, Rephaeli, Gruber and Blanco 1999) observed in Coma.

This fact should be not considered as a problem for the model we have worked out here since other alternative explanations have been proposed to fit the EUV and hard X-ray emission excesses in the framework of thermal (see Antonuccio-Delogu et al. 2000) and/or suprathermal phenomena (Ensslin et al. 1999-2000, Dogiel 1999, Sarazin and Kempner 1999, Blasi et al. 2000), respectively .

Another remarkable feature of the present model, is that neutralino annihilation can also give rise to gamma rays with continuum fluxes which are overwhelmingly due to $\pi^0 \rightarrow \gamma + \gamma$ decays. The continuum gamma-ray spectrum is given by:

$$f_\gamma(E_\gamma) = 2 \int_{E_\ell(E_\gamma)}^{M_\chi} dE_\pi (E_\pi^2 - m_\pi^2)^{-1/2} \zeta_\pi f(E_\pi) \tag{31}$$

(see,e.g., Rudaz and Stecker 1988) where the quantity $\zeta_\pi f(E_\pi)$ is derived in equation (A12) of the Appendix. We recall here that E_π is the pion energy, $E_\ell = E_\gamma + m_\pi^2/4E_\gamma$ and E_γ is the energy of the gamma-ray photon. The resulting gamma-ray luminosity is

$$L_\gamma = 4\pi n_{\chi,0}^2 \langle \sigma V \rangle_A \int_0^R dr r^2 g^2(r) f_\gamma(E_\gamma) \tag{32}$$

and yields, for Coma, a gamma-ray flux $F_\gamma(> 100MeV) = 3 \cdot 10^{-9}\ cm^{-2}s^{-1}$ (for $M_\chi = 100$ GeV; see Fig.10), which stays below the EGRET upper limit for Coma, $F_\gamma^{Coma}(> 100MeV) = 4 \cdot 10^{-8}\ cm^{-2}s^{-1}$ (Sreekumar et al. 1996).

Note that a correlation $L_\gamma \propto L_X^{(2b-1)/2b}$ (here b is the exponent of the X-ray luminosity – temperature correlation, $L_X \sim T^b$) is expected in this model with $f_g = \text{const}$, at variance with the correlation $L_\gamma \sim L_X^{1/4}$ expected in models of cosmic ray (pp) interaction in the ICM, (Colafrancesco and Blasi 1998). The different slope of the $L_\gamma - L_X$ relation will provide a way to disentangle between these two mechanisms for the production of gamma rays in galaxy clusters.

The gamma ray emission produced by $\chi\chi$ interaction extends up to energies corresponding to the neutralino mass (see Fig.11). One way to disentangle a particular

model for the cluster gamma-ray emission is provided by the future high-energy gamma-ray experiments. They will allow to observe galaxy clusters with a photon statistics sufficient to disentangle the gamma-ray spectra produced by the $\pi^0 \rightarrow \gamma + \gamma$ electromagnetic decay, as predicted either in DM annihilation models ($\chi\chi \rightarrow ff, WW \rightarrow \pi^0$) or in secondary electron models ($pp \rightarrow \pi^0$; see, e.g., Colafrancesco and Blasi 1998), from the gamma-ray emission produced by the bremsstrahlung of primary cosmic ray electrons. These observational capabilities will be available, however, in the next future. We will discuss more specifically this issue in a forthcoming paper.

Finally, we want to discuss a number of additional stringent predictions through which the model discussed here can be tested.

(i) According to the fact that DM is present in all large scale structures, we should observe radio halos in every cluster, which is not actually observed. In the framework of this paper, we have shown that radio halos can be fitted with sensitively high magnetic fields (with central values $B_0 \sim 5 \div 100$ μG). Then, only clusters which have such high magnetic fields can show a bright radio halo. All the other clusters are expected to have faint radio halos that can brighten up when there is some effect that raises the magnetic field amplitude, for example, a merging event (see the numerical simulations of K. Roettiger. 1999).

(ii) A possible problem could be given by the fact that cooling flow clusters, which have usually high magnetic field in their central cooling regions, do not show strong evidence for extended radio halos. However, if one assumes that the magnetic field in cooling flow clusters is quite peaked near the cluster center and decreases rapidly towards the outskirts, the radio halo emission predicted in the present model is a factor $\sim 10^2 \div 10^6$ lower than that of a non-cooling flow cluster with the same mass [these estimates are obtained for a Coma-like cluster using the magnetic field profile given in eq.(19) with parameters, $r_{c,B} = 0.1 h_{50}^{-1}$ Mpc and $w = 0.5 \div 2$]. Nonetheless, it remains true that our model does predict that cooling flow cluster should possess small-size, low-luminosity and low-surface

brightness radio halos.

(iii) Under the assumption that all clusters show a universal DM profile, the radio halo spectrum is basically the same unless the magnetic field configuration of the cluster is very peculiar. For example, steep radio halo spectra can be obtained mainly due to the presence of magnetic fields that decrease strongly from the cluster center.

Little is known about the presence and structure of the IC magnetic fields. Faraday rotation measurements (Vallee et al. 1986, 1987) give a lower estimate of the magnetic field in small scale regions of the cluster (Dolag et al. 1999), and we could have to deal with large scale IC magnetic fields that are lower than those ($B_0 \sim 5 \div 100$ μG, $B_{uniform} \sim 1 \div 3$ μG) required by the present model to explain radio halos. However, even though the magnetic field are not so strong in clusters, the present model certainly yields a natural explanation for the origin of the seed high-energy electrons, which are a necessary input for any model of radio halo (and relic) formation. The diffuse radio emission due to such a population of seed electrons could then be boosted by the amplification of the IC magnetic field subsequent to a strong cluster merger (Roettiger 1999), or the seed electrons could be reaccelerated by intracluster turbulence (Deiss et al. 1997, Eilek and Weatherall 1999, Brunetti et al. 1999).

While at the moment, we observe radio halos in more than 20 clusters at different redshifts, the definite test for the theory of the radio halo origin proposed here is committed to obtain a larger, unbiased survey of galaxy clusters through high radio sensitivity observations. This search should be complemented with the search for gamma-ray emission from galaxy clusters whose predicted intensity is matched by the sensitivities of the next generation gamma-ray experiments (GLAST, AGILE, MAGIC, VERITAS, ARGO, STACEE).

In conclusion, we want to emphasize that the astrophysical expectations from the $\chi\chi$ annihilation are consistent, at the moment, with the constraints set by all the available

observations on clusters containing radio halos. The astrophysical and fundamental physics requirements on the model discussed here are stringent, but still well allowed. It is also appealing, in these respects, to expect that some astrophysical features of galaxy clusters might give information on the fundamental properties of the DM particles.

Aknowledgments. The authors acknowledge several stimulating discussions with P. Lipari, D. Fargion, A. Fabian and L. Feretti.

A. APPENDIX. The production spectrum of high-energy electrons

In this Appendix we will derive an analytical approximation for the source spectrum of electrons resulting from the decay products of $\chi\chi$ annihilation. Here we will refer mainly to the analytical approaches of Rudaz and Stecker (1988; hereafter RS) and of Kamionkowski and Turner (1991; hereafter KT) who gave analytical approximations of the positron source functions for models in which neutralinos annihilate mainly into fermions ($\chi\chi \rightarrow ff$) or gauge bosons ($\chi\chi \rightarrow WW$) , respectively. In the following, we derive the electron source spectra for generic values of the neutralino number density, $n_\chi(r)$, and annihilation cross section, $\langle\sigma V\rangle_A$.

A.1. Fermion dominated annihilation

Following RS, we consider three main sources of $e^\pm$ from $\chi\chi$ annihilation: (P1) first generation, prompt electrons with a continuum spectrum; (P2) second generation, prompt electrons; (π) electrons produced from the decay of $\pi^\pm$. The electron source spectrum, $Q(E,r)$, can be written as the sum of these three components

$$Q_{ff}(E,r) = Q_{P1}(E,r) + Q_{P2}(E,r) + Q_\pi(E,r) \ . \tag{A1}$$

For a neutralino with mass $M_\chi = 100$ GeV, the first generation source spectrum takes contributions mainly from $b \rightarrow e, c \rightarrow e, \tau^\pm \rightarrow e^\pm$ (see RS). Taking into account the different energy distributions of the previous decays, the first generation electron spectrum is found to be well approximated by

$$Q_{P1}(E,r) = n_\chi^2 \langle\sigma V\rangle_A \zeta_1 f_1(E) \tag{A2}$$

with $\zeta_1 \approx 0.6/(kM_\chi)$ and $k \approx 0.7$.

The function $f_1(E)$ is given by

$$f_1(x) = \frac{0.17}{31} f_\tau(x) + 0.13 \times \frac{3}{31} f_c(x) + 0.1 \times \frac{27}{31} f_b(x) \tag{A3}$$

where

$$f_\tau(x) = f_b(x) = \frac{5}{3} + \frac{4}{3}x^3 - 3x^2 \tag{A4}$$

and

$$f_c(x) = 2\Big(1 + 2x^3 - 3x^2\Big) \tag{A5}$$

in terms of the adimensional quantity $x = E/M_\chi$. In eq.(A3) we replace the values assumed by RS for the leptonic decay branching ratios with the present values taken from the Particle Data Group (Groom et al. 2000). Neglecting the differences between f_τ, f_b and f_c, the source function Q_{P1} – as noticed by RS – can be approximated by

$$Q_{P1}(E, r) \approx 0.11 n_\chi^2 \langle \sigma V \rangle_A \cdot f(E) \tag{A6}$$

where

$$f(E) = \frac{1}{kM_\chi} \theta(kM_\chi - E) \tag{A7}$$

where the function $\theta(kM_\chi - E)$ is the Heaviside function. The source function $Q_{P1}(E, r)$ is basically constant up to $E \approx kM_\chi$ and then drops to zero for higher energies (see Fig.1).

The second generation source spectrum (arising from the leptonic decays in the final states of the first generation decays) is found to be well approximated by:

$$Q_{P2}(E, r) = n_\chi^2 \langle \sigma V \rangle_A \zeta_2 f_2(E) \tag{A8}$$

with

$$f_2(E) = \frac{1}{k^2 M_\chi} ln\Big[\frac{k^2 M_\chi}{E}\Big] \tag{A9}$$

where, again, $k \approx 0.7$ and

$$\zeta_2 \approx \frac{0.17}{31} + 0.13 \times \frac{3}{31} + 0.1 \times 2 \times \frac{27}{31} \ . \tag{A10}$$

This source function goes rapidly to zero for $E \to k^2 M_\chi \approx M_\chi/2$ (see Fig.1). Again, in eq.(A10) we replace the values assumed by RS for the leptonic decay branching ratios with the present values taken from the Particle Data Group (Groom et al. 2000).

Following RS, we find that the source spectrum from $\pi^\pm$ decay is found to be well approximated by:

$$Q_\pi(E, r) = n_\chi^2 \langle \sigma V \rangle_A \zeta_\pi f_\pi(E) \tag{A11}$$

with

$$f_\pi(E) = e^{-0.68E} + 0.115 e^{-0.276E} \tag{A12}$$

and $\zeta_\pi \approx 1.74(100 \text{ GeV}/M_\chi)$.

The three source functions for P1, P2 and π contributions together with the total source function are plotted in Figs.1 and 2.

A.2. Gauge boson dominated annihilation

In addition to the electron produced by the direct decays of vector bosons (typical energy of $\sim M_\chi/2$) there is a continuum spectrum of electrons at $E \lesssim M_\chi/2$ which are produced as secondary decay products ($W^\pm \to \tau^\pm \to e^\pm$, $W^\pm \to c \to e^\pm$) and from the decays of charged pions produced in hadronic decays of the $W^\pm$ and Z^0 bosons. Since the electron distributions arising from the W and the Z bosons are qualitatively similar, we will restrict our analysis to the W case. Following KT, the source distribution function of secondary-decay electrons, integrated over the quark and lepton energies, is

$$Q_{W,\mu,\tau,c}(E, r) = n_\chi^2 \langle \sigma V \rangle_A \zeta_{W,\mu,\tau,c} f_{W,\mu,\tau,c}(E) \tag{A13}$$

where

$$\zeta_{W,\mu,\tau,c} = B_{W\to\mu} + 0.17 B_{W\to\tau} + 0.13 B_{W\to c} \tag{A14}$$

and

$$f_{W,\mu,\tau,c}(E) = \left\{ \begin{array}{ll} \frac{1}{kM_\chi\delta} ln\left[\frac{(1+\delta)}{(1-\delta)}\right] & \text{for } E \leq \frac{kM_\chi}{2}(1+\delta), \\ \frac{1}{kM_\chi\delta} ln\left[\frac{kM_\chi(1+\delta)}{2E}\right] & \text{for } \frac{kM_\chi}{2}(1+\delta) \leq E \leq \frac{kM_\chi}{2}(1+\delta), \\ 0 & \text{for } E \geq \frac{kM_\chi}{2}(1+\delta), \end{array} \right\} \tag{A15}$$

In this expression, $\delta = [1 - (M_W/M_\chi)^2]^{1/2}$ with $M_W = 80$ GeV being the W boson mass. Adopting values $B_{W\to\mu} = 0.11$, $B_{W\to\tau} = 0.11$ and $B_{W\to c} = 0.34$ for the previous branching ratios, we obtain $\zeta_{W,\mu,\tau,c} \approx 0.1729$.

The hadronization of quarks from gauge boson decays results in a shower of charged pions which eventually decay into electrons ($\pi^\pm \to \mu^\pm \to e^\pm$). Following KT, the source function for the pion-produced electrons, integrated over the quark energy distribution, writes

$$Q_{W,\pi}(E,r) = n_\chi^2 \langle\sigma V\rangle_A \zeta_{W,\pi} f_{W,\pi}(E) \tag{A16}$$

where $\zeta_{W,\pi} \approx 2/3$ and

$$f_{W,\pi}(E) = \frac{1}{M_\chi\delta} \int_{E_{min}}^{E_{max}} dE' \left[93 e^{-68E/E'} + 56 e^{-27.6E/E'}\right] \tag{A17}$$

where $E_{min} = M_\chi(1-\delta)/2$ and $E_{max} = M_\chi(1+\delta)/2$. The total source function for this case writes

$$Q_{WW}(E,r) = Q_{W,\mu,\tau,c}(E,r) + Q_{W,\pi}(E,r) \tag{A18}$$

and is compared to the source function $Q_{ff}(E,r)$ in Figs.1 and 2.

REFERENCES

Antonuccio-Delogu et al. 2000, in Proceedings of the Moriond Meeting *Energy Densities in the Universe*, Tran-Tan van et al Eds., in press

Arnaud, M. and Evrard, A.E. 1999, MNRAS, 305, 631

Bahcall, N. 1999, preprint astro-ph/9901076

Baltz, E.A. and Edsjö 1998, preprint astro-ph/9808243

Bengtsson, H.U. et al. 1990, Nucl. Phys. B, 346, 129

Blasi, P., 1999, ApJ, 525, 603

Blasi, P. and Colafrancesco, S. 1999, Astroparticle Physics, 12, 169

Bottino, A., Donato, F., Fornengo, N. and Salati, P. 1998, preprint astro-ph/9804137

Brunetti, G., Feretti, L., Giovannini, G. and Setti, G. 1999, in Proceedings of the Ringberg Workshop 'Diffuse Thermal and Relativistic Plasma in Galaxy Clusters', MPE Report 271, p.263

Cavaliere, A. And Fusco-Femiano, R. 1976, A&A, 49, 137

Chardonnet, P. et al. 1995, ApJ, 454, 774

Chardonnet, P., Mignola, G., salati, P. and Taillet, R. 1996, Phys.Lett. B, 384, 161

Colafrancesco, S., Mazzotta, P. and Vittorio, N. 1997, ApJ, 488, 566

Colafrancesco, S. and Blasi, P. 1998, Astroparticle Physics, 9,227

Colafrancesco, S. 1999, in Proceedings of the Ringberg Workshop 'Diffuse Thermal and Relativistic Plasma in Galaxy Clusters', MPE Report 271, p.295

Colafrancesco, S., ApJ, submitted

David, L.P. et al. 1993, ApJ, 412, 479

Deiss, B. et al. 1997, A&A, 321, 55

Dennison, B. 1980, ApJ, 239, L93

Dogiel, V. in Proceedings of the Ringberg Workshop 'Diffuse Thermal and Relativistic Plasma in Galaxy Clusters', MPE Report 271, p.259

Dolag, K., Bartelmann, M. and Lesch, H. 1999, A&A, 348, 351

Edsjö, J. 1997, PhD Thesis (hep-ph/9704384)

Eilek, J. and Weatherall, J.C. 1999, in Proceedings of the Ringberg Workshop 'Diffuse Thermal and Relativistic Plasma in Galaxy Clusters', MPE Report 271, p.249

Ellis, J. et al. 1989, Phys. Lett. B, 214, 403

Ellis, J., Falk, T., Ganis, G., and Olive, K.A. 2000, preprint hep-ph/0004169

Ensslin, T.A., Lieu, R. and Biermann, P.L. 1999, A&A, 344, 409

Ensslin, T.A. and Kaiser, C. 2000, preprint astro-ph/0001429

Feretti, L. and Giovannini, G. 1997, in 'A New Vision of an Old Cluster: Untangling Coma Berenices', F. Durret et al. Eds., in press (astro-ph/9709294)

Feretti, L. 1999, in Proceedings of the Ringberg Workshop 'Diffuse Thermal and Relativistic Plasma in Galaxy Clusters', MPE Report 271, p.3

Friaca, A.C.S. and Goncalves, D.R. 1998, astro-ph/9811264

Fusco-Femiano, R. et al. 1999, ApJ, 513, L24

Giovannini, G. et al. 1993, ApJ, 406, 359

Giovannini, G. and Feretti, L. 1996, in 'Extragalactic Radio Sources', R. Ekers et al. Eds, p.333

Giovannini, G., Tordi, M. and Feretti, L. 1999, preprint astro-ph/9904210

Golubkov, Yu.A., Konoplich, R.V. 1998, Yad.Fiz.61:675, Phys.Atom.Nucl.61:602

Groom, D.E. et al. 2000, the Particle Data Group, The European Physical Journal, C15,1 (http://pdg.web.cern.ch/pdg/)

Haber, H.E. and Kane, G.L. 1985, Phys. Rep. 117, 75

Jaffe, W.J. 1977, ApJ, 212, 1

Jones, C. and Forman, W. 1999, ApJ, 511, 65

Jungman, G., Kamionkowski, M., and Griest, K. 1996, Phys. Rep. 267, 195

Kaastra, J.S., Lieu,R., Mittaz, J., Bleeker, J., Mewe, R., Colafrancesco, S. and Lockman, F. 1999, ApJ, 519, L119

Kamionkowski, M. and Turner, M.S. 1991, Phys. Rev. D, 43, 1774 (KT)

Kaplinghat, M., Knox, L. and Turner, M.S. 2000, preprint astro-ph/0005210

Kolb, E.W. and Turner, M.S. 1990, 'The Early Universe', Addison-Wesley)

Kronberg, P.P. 1994, Rep. Prog. Phys., 57, 325

Liang, H. 1999, in Proceedings of the Ringberg Workshop 'Diffuse Thermal and Relativistic Plasma in Galaxy Clusters', MPE Report 271, p. 33

Liang, H., Hunstead, R.W., Birkinshaw, M. and Andreani, P. 2000, preprint astro-ph/0006072

Lieu, R. et al. 1996, Science, 274, 1335

Mohr, J. 2000, preprint astro-ph/0004244

Navarro, J., Frenk, C. and White, S.D.M. 1997, ApJ, 490, 493 (NFW)

Owen, F., Morrison, G. and Voges, W. 1999, in Proceedings of the Ringberg Workshop 'Diffuse Thermal and Relativistic Plasma in Galaxy Clusters', MPE Report 271, p. 9

Peebles, J.E. 1980, 'The Large Scale Structure of the Universe', Princeton Univ. Press

Rephaeli, Y., 1979, ApJ, 227, 364

Rephaeli, Y., Gruber, D. and Blanco, P. 1999, ApJ, 511, L21

Roland, J. et al. 1981, A&A, 100, 7

Roettiger, K. 1999, in Proceedings of the Ringberg Workshop 'Diffuse Thermal and Relativistic Plasma in Galaxy Clusters', MPE Report 271, p. 231

Rudaz, S. and Stecker, F.W. 1988, ApJ, 325, 16 (RS)

Sarazin, C.L. 1988, 'X-ray Emission from Clusters of Galaxies', Cambridge Univ. Press.

Sarazin, C.L. and Kempner, J.C. 1999, ApJ, 533, 73

Sarazin, C.L. 1999, ApJ, 520, 529

Schlikaiser, R. et al. 1987, A&A, 227, 236

Silk, J. and Srednicki, M. 1984, Phys.Rev.Lett., 53, 624

Silk, J. and Gondolo, P. 1999, preprint astro-ph/9906391

Sreekumar, P. et al. 1996, ApJ, 464, 628

Stecker, F. and Tylka, A. 1989, ApJ, 336, L51

Takizawa, M. and Naito, T. 2000, ApJ, 535, 586

Turner, M. and Wilczek, F. 1990, Phys.Rev.D, 42, 1001

Vallee, J.P. et al. 1986, A&A, 156, 386

Vallee, J.P. et al. 1987, ApL, 25, 181

Vestrand, W.T. 1987, ICRC Proc. OG 3.1-5, 97

Weinberg, S. 1972, 'Gravitation and Cosmology', (Wiley and Sons)

Wu, X-P., Xue, Y-J. and fang, L-Z. 1999, ApJ, in press (astro-ph/9905106)

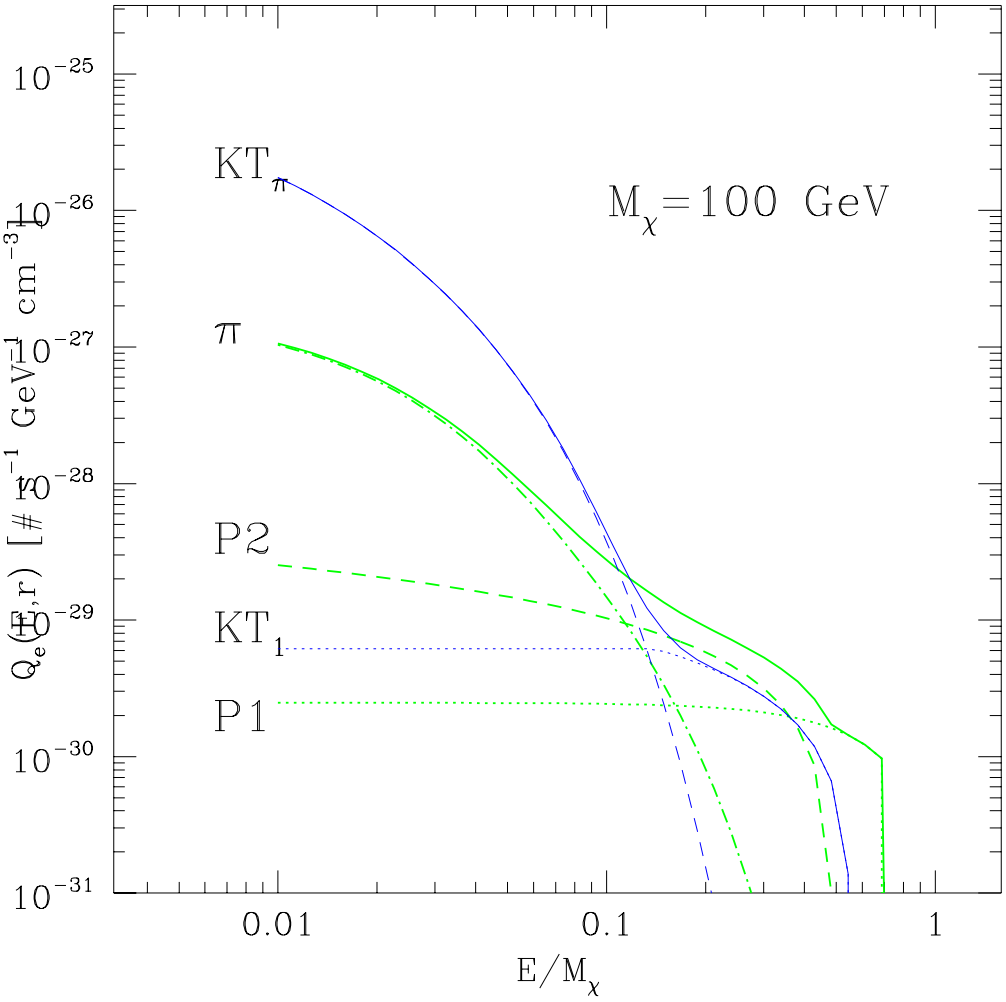

Fig. 1.— The source spectrum for a model in which fermions dominate the neutralino annihilation products ($\chi\chi \to ff$): first generation, prompt electrons (P1), second generation, prompt electrons (P2) and secondary electrons produced in the decay of charged pions (π). The light solid curve is the total source spectrum for this case.

We also show the source spectra for the model in which gauge bosons dominate the annihilation. The contributions from the decays ($W^\pm \to \tau^\pm \to e^\pm$, $W^\pm \to c \to e^\pm$) and from the decays of charges pions produced in hadronic decays of $W^\pm$ and Z^0 bosons are labelled KT_1 (light dotted curve) and KT_π (light dashed curve), respectively. The light solid curve is the total source spectrum for the case ($\chi\chi \to WW$). A neutralino density $n_\chi = 1$ cm^{-3} and annihilation cross section $\langle \sigma V \rangle_A = 10^{-27}$ cm^3 s^{-1} have been used in this plot.

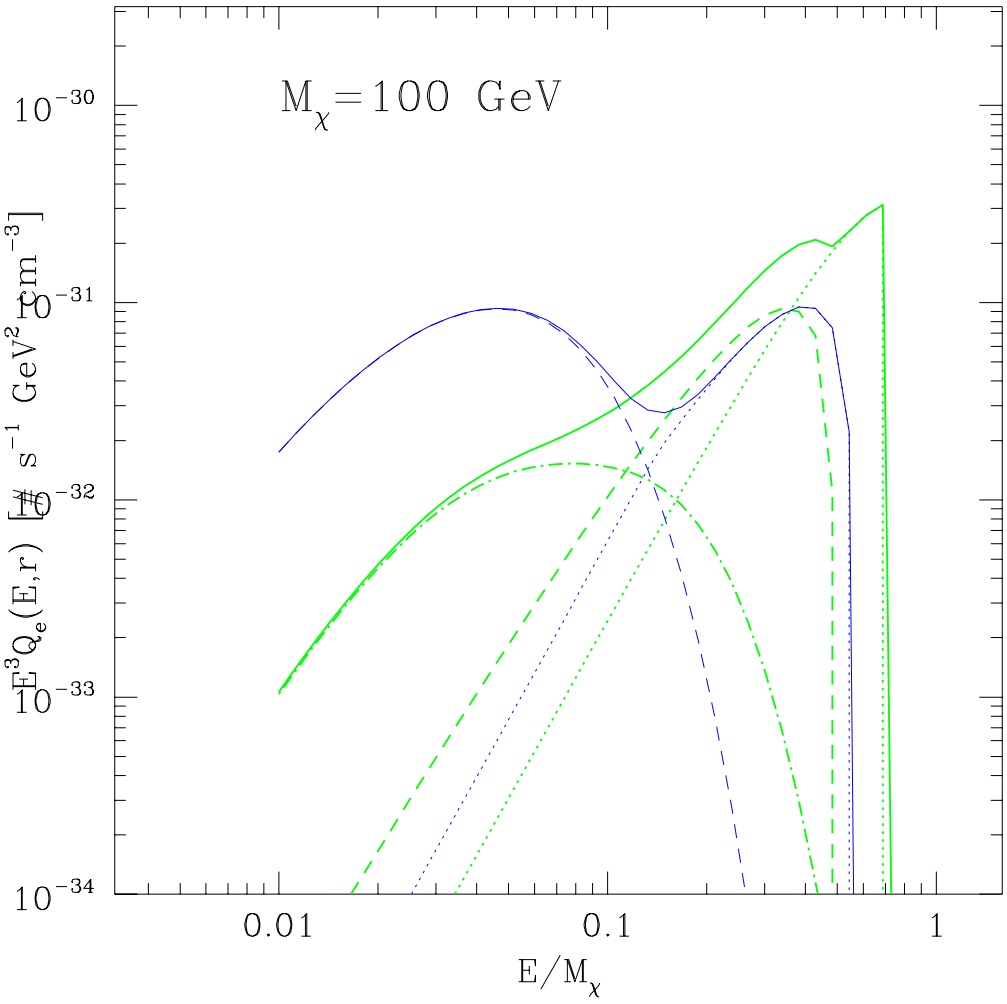

Fig. 2.— The quantity $E^3Q_e(E,r)$ is shown for the source spectra plotted in Fig.1. Curves are labelled as in Fig.1.

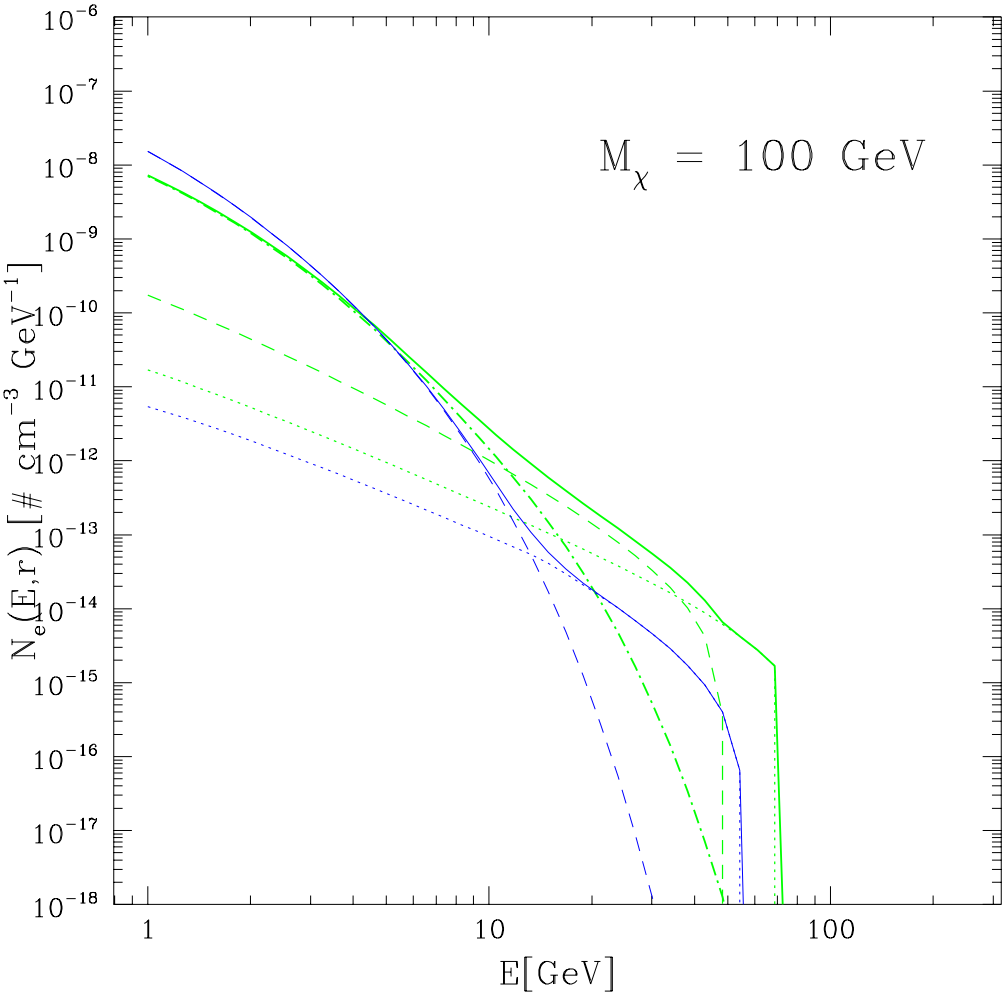

Fig. 3.— The overall equilibrium spectrum $N_e(E, r)$ of the electrons whose source functions are shown in Fig. 1. The equilibrium spectra are calculated separately for each source electron population given in Fig.1. The heavy and light solid curves are the total equilibrium spectra for the cases $\chi\chi \rightarrow ff$ and $\chi\chi \rightarrow WW$, respectively. A neutralino with mass $M_\chi = 100$ GeV has been adopted.

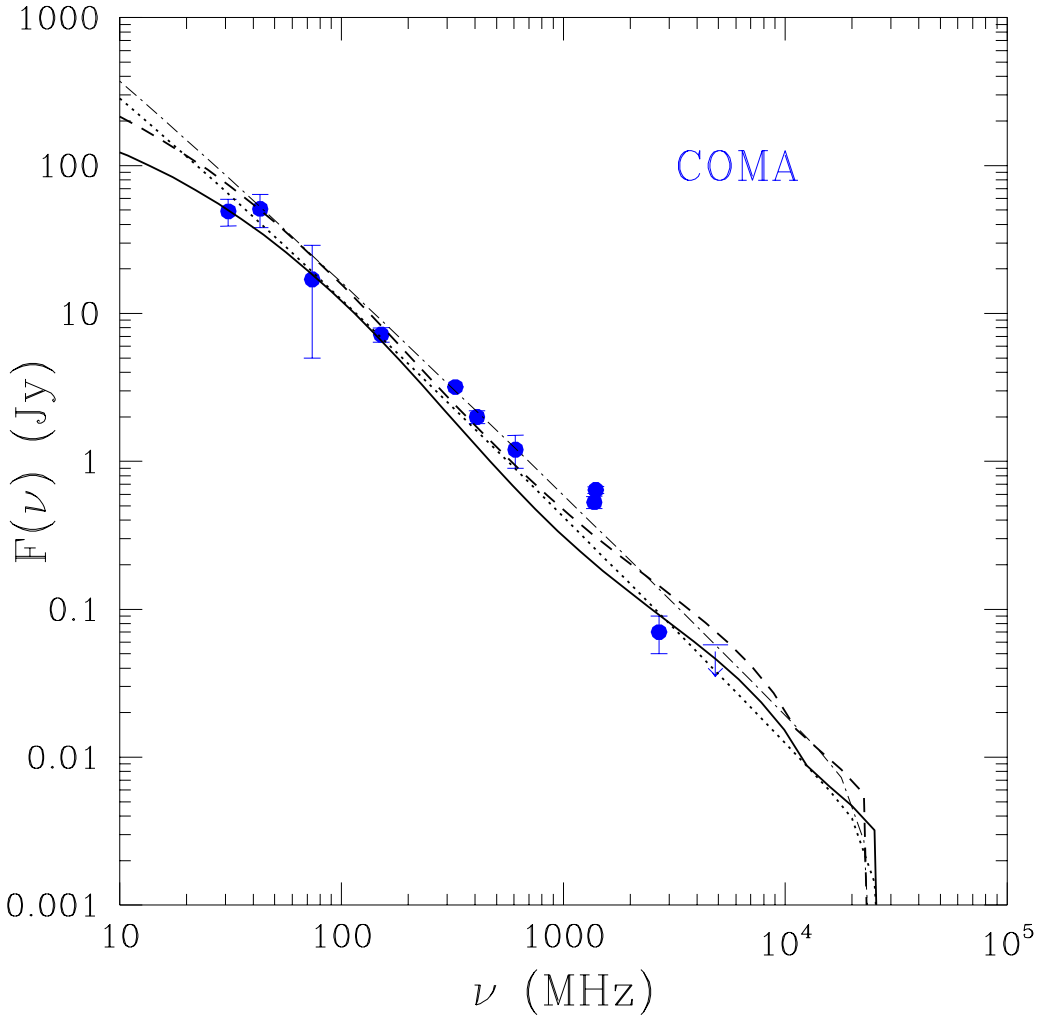

Fig. 4.— The Coma radio halo spectrum predicted in a model in which χ annihilation is dominated by fermions ($\chi\chi \to ff$). The curves are for a uniform magnetic field of $B_{uniform} = 1.3\mu$G (dashed) and for a radially decreasing magnetic field with central value $B_0 = 8\mu$G (solid). We also show the radio halo spectra obtained from a power-law approximation, $Q_e \sim E^{-1.9}$ to the true source spectrum shown in Fig.1 with $B_{uniform} = 1.3\mu$G (dot-dashed) and $B_0 = 8\mu$G (dotted). A constant core profile with $r_c = 0.4h_{50}^{-1}$ Mpc, $\beta = 0.76$ has been adopted. The radio halo emission has been integrated out to $1.3h_{50}^{-1}$ Mpc. Data are taken from Deiss et al. (1997).

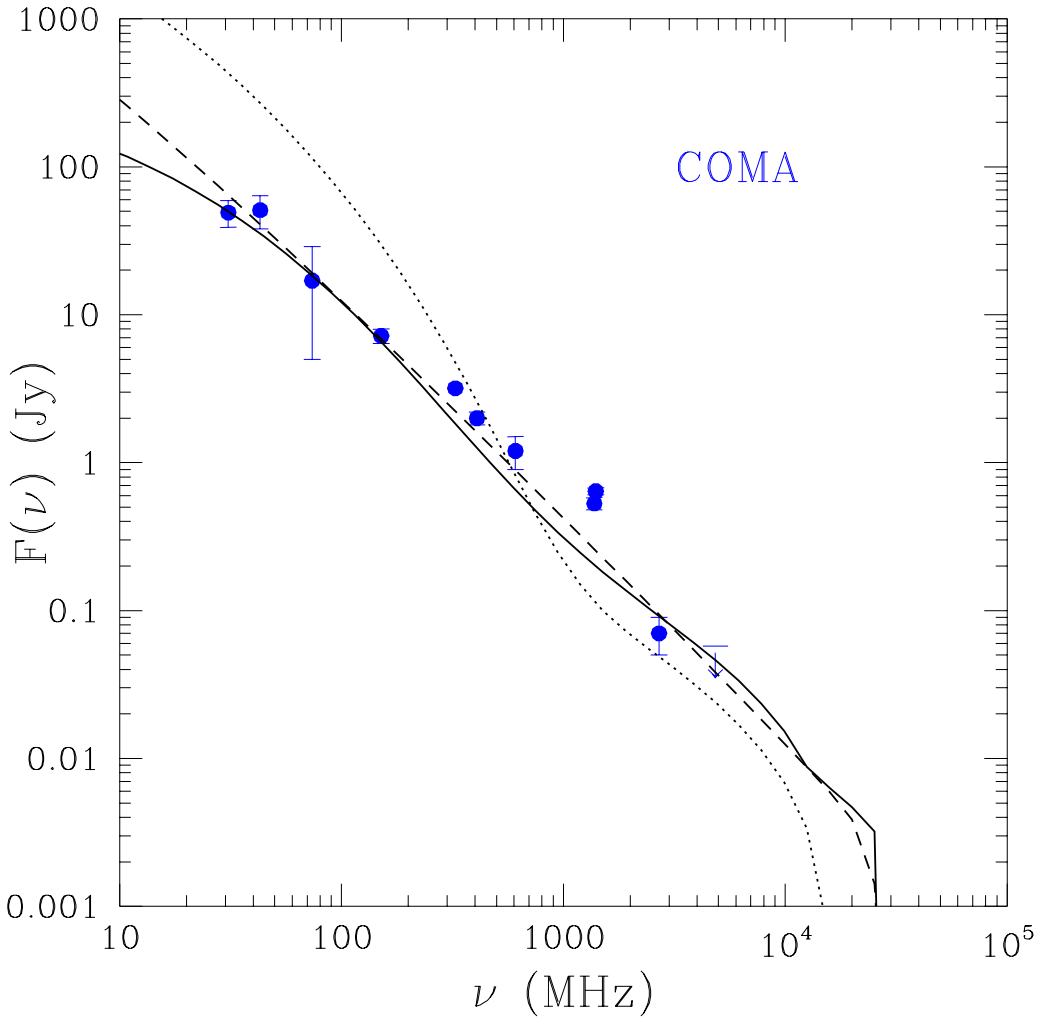

Fig. 5.— The Coma radio halo spectrum predicted in a model in which χ annihilation is dominated by fermions ($\chi\chi \rightarrow ff$; solid curve) is compared to the model in which annihilation is dominated by higgsinos ($\chi\chi \rightarrow WW$; dotted curve). The power-law approximation for the case $\chi\chi \rightarrow ff$ is also shown (dashed curve). The curves are plotted for a radially decreasing magnetic field with central value $B_0 = 8\mu$G. A constant core profile with $r_c = 0.4h_{50}^{-1}$ Mpc, $\beta = 0.76$ has been adopted. The radio halo emission has been integrated out to $1.3h_{50}^{-1}$ Mpc. Data are taken from Deiss et al. (1997).

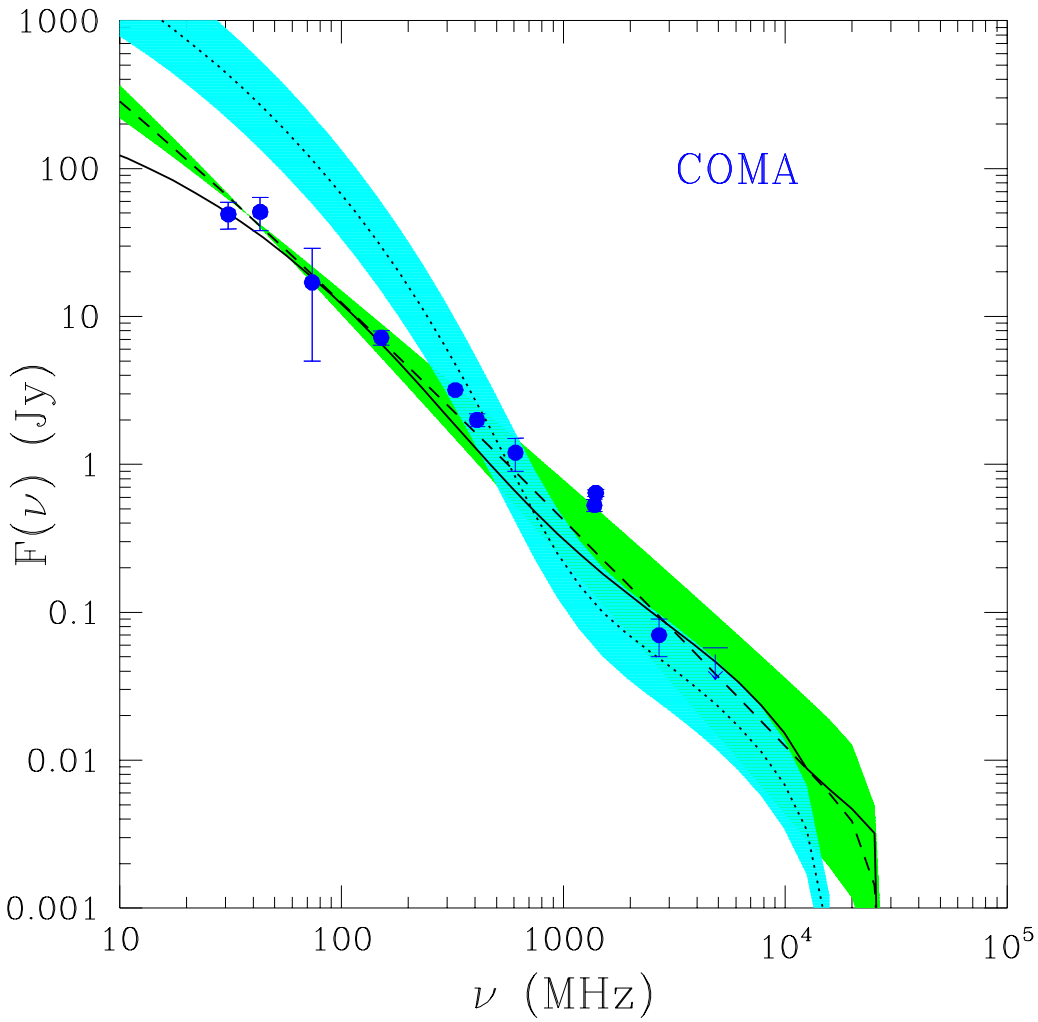

Fig. 6.— In this figure we show how the uncertainties in the electron source spectrum reflect on the shape of the radio halo spectrum of Coma. Shaded areas enclose radio halo spectra evaluated considering both an uncertainty of a factor ±2 in normalization and ±10% in the slope of the source spectra. Dark gray region refers to the $\chi\chi \to ff$ case and pale gray region to the $\chi\chi \to WW$ case. Curves are labelled as in Fig.5.

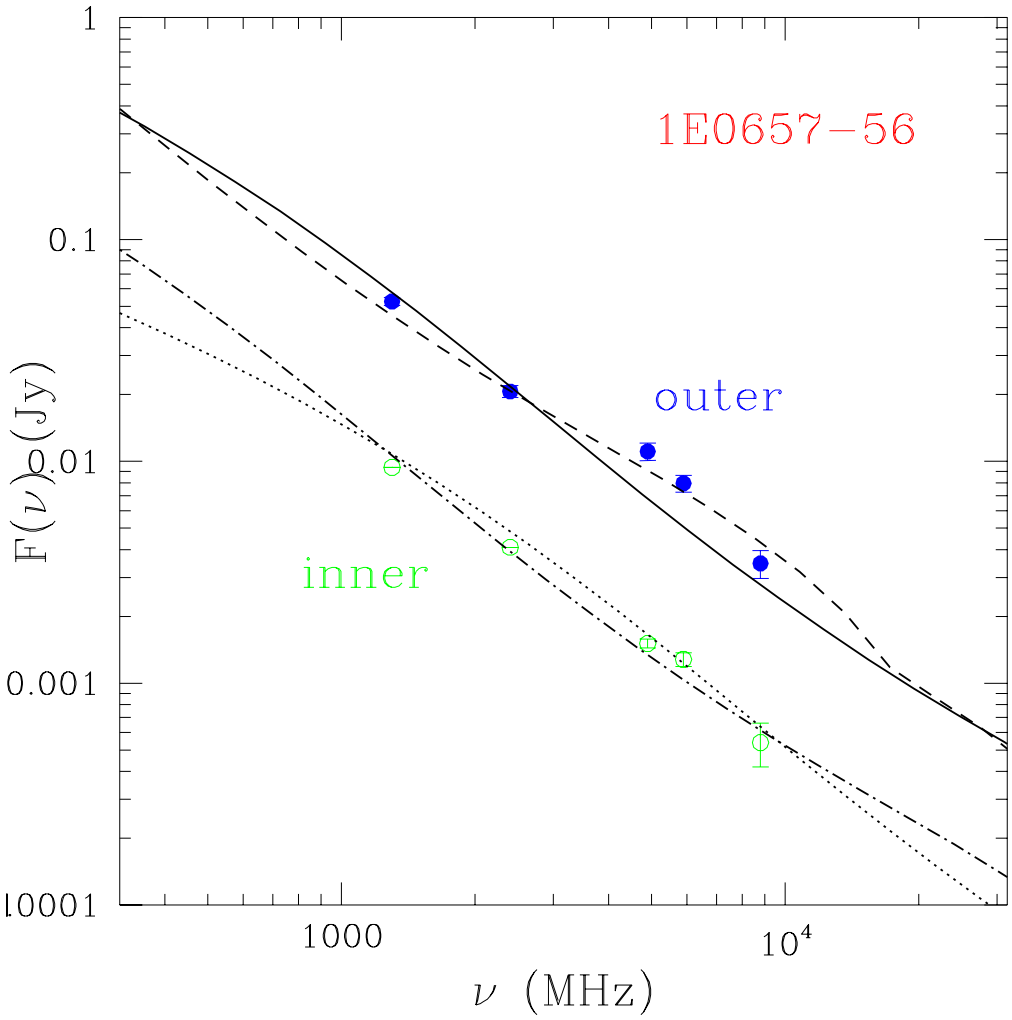

Fig. 7.— The radio halo spectrum of the cluster 1E0657-56 in the inner (empty circles) and outer (filled circles) regions. Dashed and dot-dashed curves are for a uniform field $B_{uniform} = 2\mu$G and $B_{uniform} = 9\mu$G, respectively. Solid and dotted curves are for a magnetic field with a radial dependence $B = B_0\Big[1 + (r/r_{c,B})^2\Big]^{-0.5}$ with a central amplitude $B_0 = 100\mu$G and $B_0 = 90\mu$G, respectively. Curves are shown for a model in which neutralino annihilation is dominated by fermions ($\chi\chi \rightarrow ff$). Constant core density profiles have been adopted here with parameters $R_{halo} = 2h_{50}^{-1}$ Mpc, $r_c = 0.38h_{50}^{-1}$ Mpc, $\beta = 0.7$ and $n_{\chi,0} = 9 \cdot 10^{-3}$ cm^{-3} for the outer region and $R_{halo} = 0.6h_{50}^{-1}$ Mpc, $r_c = 0.08h_{50}^{-1}$ Mpc, $\beta = 0.49$ and $n_{\chi,0} = 9 \cdot 10^{-3}$ cm^{-3} for the inner region (see Liang et al. 2000). Data are from Liang et al. (2000).

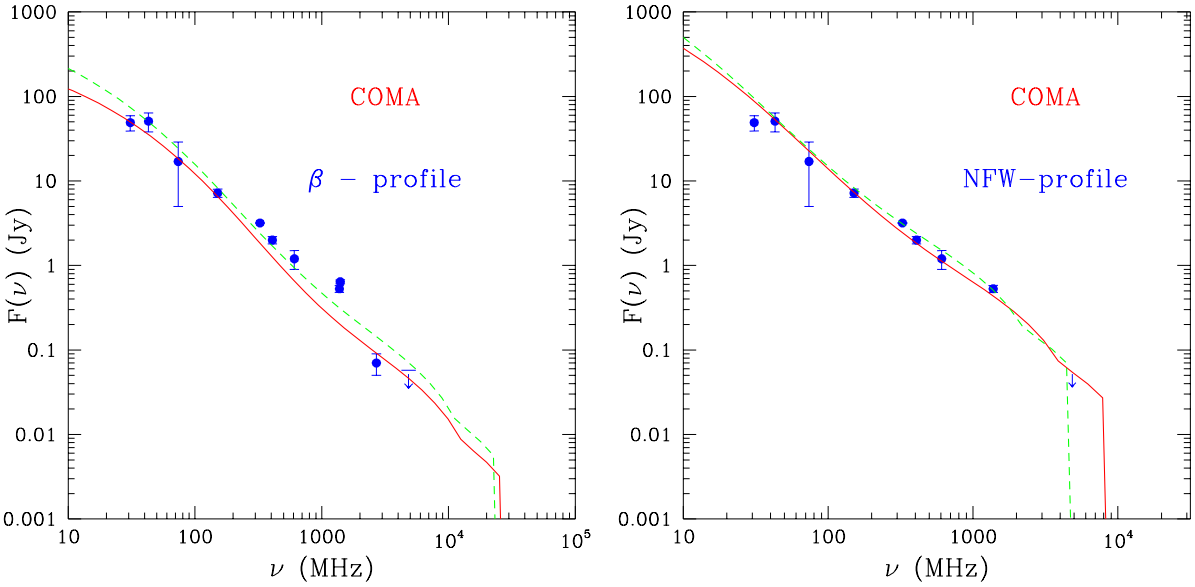

Fig. 8.— The Coma radio halo spectrum for a constant core beta-profile (left panel) and for a NFW profile (right panel). Dashed and solid curves refer to the $B_{uniform} = 1.3\mu$ G and $B_0 = 8\mu$G for the beta-profile (left panel) and to $B_{uniform} = 0.45\mu$ G and $B_0 = 1.4\mu$G for the NFW profile (right panel). A neutralino annihilation model $\chi\chi \rightarrow ff$ has been assumed. Data are from Deiss et al. (1997).

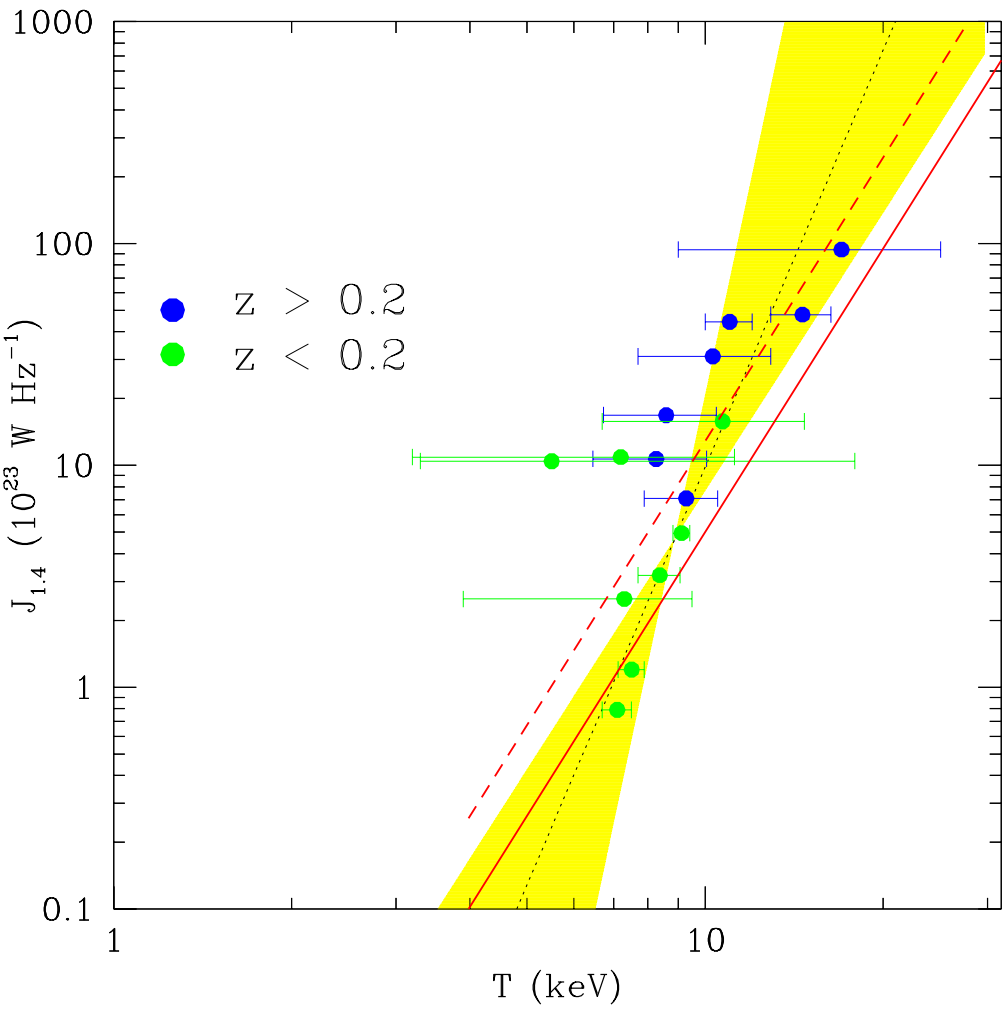

Fig. 9.— The $J_{1.4} - T$ correlation is shown for the radio halo clusters at $z > 0.2$ (dark dots) and at $z < 0.2$ (gray dots). The dotted line is the best fit power-law to the data (the shaded area contain the uncertainty region of the best fit points, see Section 6 for details). The heavy lines are the relations $J_{1.4} \sim T^{4.25}$ expected in the neutralino annihilation model discussed in the paper and are evaluated at $z = 0$ (solid) and at $z = 0.25$ (dashed), respectively. data are taken from Feretti (1999), Giovannini et al. (1999), Liang (1999), Owen et al. (1999).

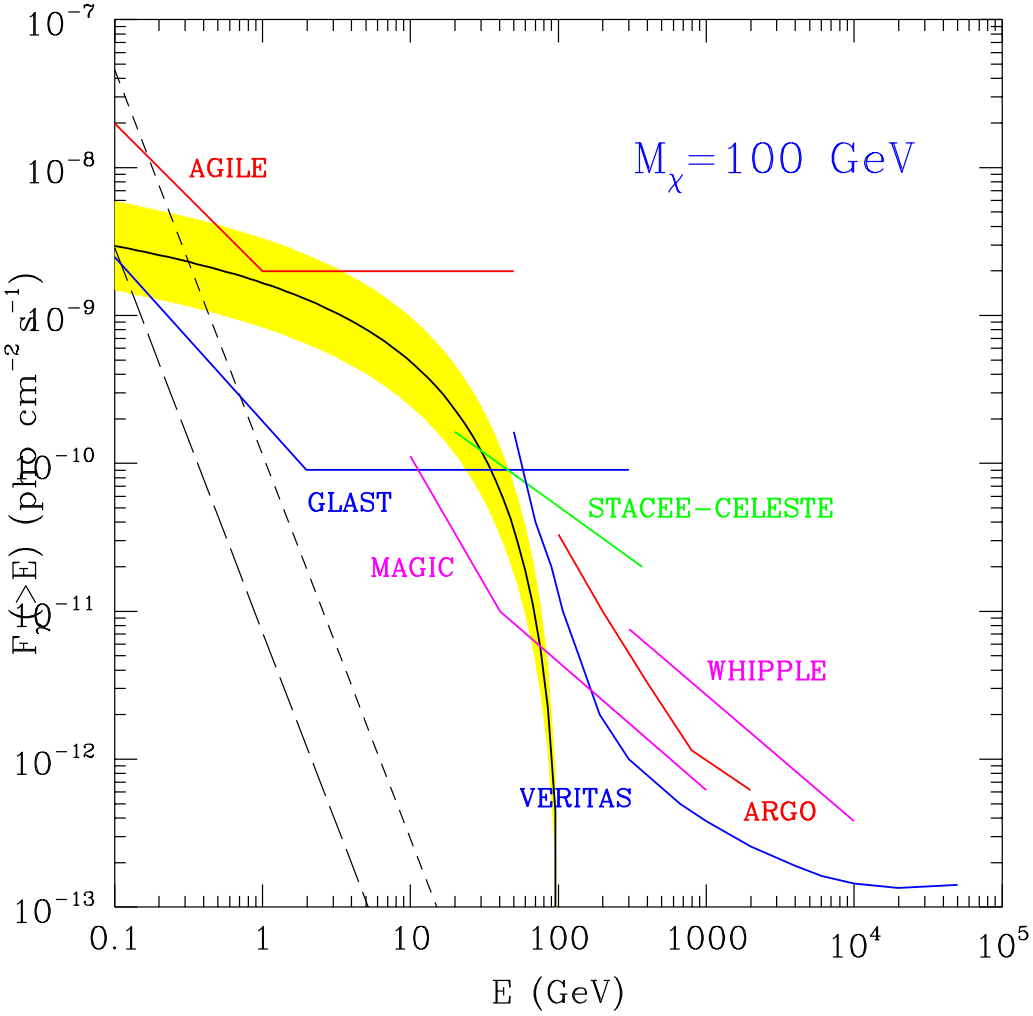

Fig. 10.— The gamma-ray emission predicted from $\chi\chi$ annihilation in Coma (solid curve) is compared to the sensitivities of the operating and planned gamma ray experiments. A neutralino with mass $M_\chi = 100$ GeV has been assumed. The shaded area shows the uncertainty in the gammma-ray spectrum due to an uncertainty of a factor 2 in the normalization of the π^0 source spectrum (see Section 3 for details). The short and long dashed curves refer to the gamma ray emission produced by relativistic bremmstrahlung of a population of primary cosmic rays and are calculated using the formula given in Sreekumar et al. (1996) for two choices of the Coma magnetic field $B = 0.3\mu$G and $B = 1\mu$G, respectively.

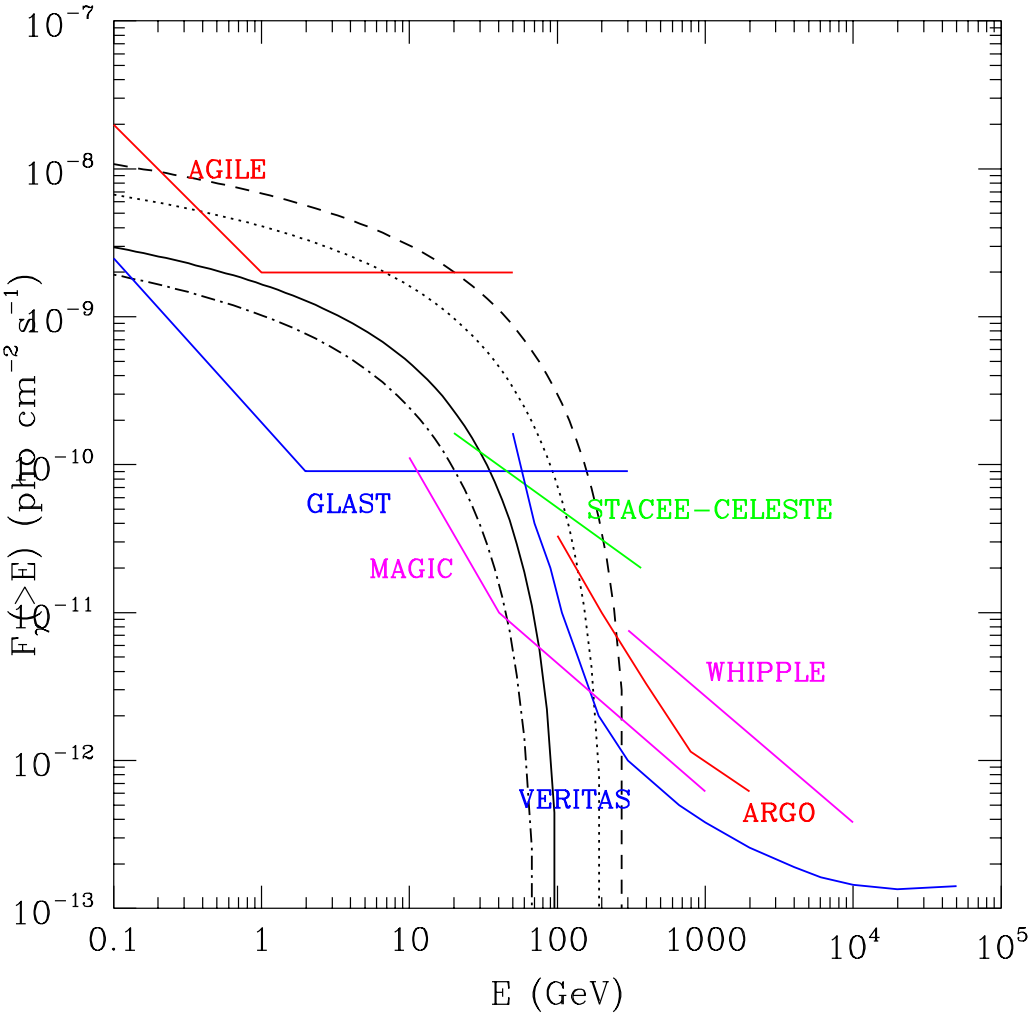

Fig. 11.— The gamma-ray emission predicted from $\chi\chi$ annihilation in galaxy clusters (solid curve) calculated for different neutralino masses: $M_\chi = 70$ GeV (dot-dashed curve), $M_\chi = 100$ GeV (solid curve), $M_\chi = 200$ GeV (dotted curve) and $M_\chi = 300$ GeV (dashed curve). The sensitivities of the operating and planned gamma ray experiments are also shown. Combined gamma ray observations of clusters from ~ 1 GeV to 500 GeV can clearly determine the neutralino mass from both the intensity of the spectrum and its high-energy cutoff (see Section 7 for details).